Master of Science in Chemical Sciences   Chemistry & Biochemistry

Summer 7-29-2015

The Role of EphA Receptor Signaling in Neuroblast Survival During In Vitro Differentiation

Tasia M. Nabors
Kennesaw State University

Follow this and additional works at: http://digitalcommons.kennesaw.edu/mscs_etd

Part of the Chemistry Commons

THE ROLE OF EPHA RECEPTOR SIGNALING IN

NEUROBLAST SURVIVAL DURING IN VITRO DIFFERENTIATION

by

Tasia Marie Nabors

Bachelor of Science

Kennesaw State University, 2007

_____

Submitted in Partial Fulfillment of the Requirements

For the Degree of Master of Science in the

Department of Chemistry and Biochemistry

Kennesaw State University

July 29th 2015

\---   \--
Committee Chair   Graduate Program Coordinator

\---   \--
Committee Member   Department Chair

\---   \--
Committee Member   College Dean

ACKNOWLEDGEMENTS

TABLE OF CONTENTS

ABSTRACT

Mouse embryonic stem cells can be differentiated into multiple cell types and can serve as an excellent model for studying developmental processes in vitro. In particular, stem cells can be differentiated into forebrain-like neurons, allowing investigation of nervous system development at single cell resolution. Eph receptor tyrosine kinases and their ephrin ligands play a critical role during in vivo cortical development, particularly during axon guidance. Preliminary data has shown that EphRs and ephrins are expressed during in vitro differentiation. In addition, we see EphA7 localization at the face of neural rosettes, where it co-expresses with markers of neuroblast identity. However, the role of Eph receptors and ephrins in neurogenesis is not well understood.

Previous literature had shown that ephrin-A5 and EphA7 can function to balance cortical apoptosis during embryogenesis. We hypothesized that EphR/ephrin signaling may be required to balance apoptosis during in vitro neural development. A monolayer differentiation protocol was used to generate cells of forebrain fate at high yield. RNAi knockdown of EphA3, EphA4, and EphA7, was used to identify which Eph receptor was contributing to the apoptotic effect individually. It was found that transient knockdown of EphA3 and EphA4 fail to cause changes in apoptosis levels. However, knockdown of EphA7 at differentiation days 4 through 8 lead to a reduction in apoptosis suggesting that EphA7 can positively regulate cell death during differentiation. These data confirm that in vivo developmental events such as apoptosis can be modeled in an in vitro system. The innovative methods developed throughout the process of this research project may eventually prove to be useful in the analysis of other neurodevelopmental processes.

Key Words: embryonic stem cell, in vitro differentiation, neurogenesis, ephrin, Eph receptor, apoptosis, siRNA, cell sorter, transfection, flow cytometry.

Abbreviations:

mESC: mouse embryonic stem cell

ICM: inner cell mass

EphR: Erethropoeitin-producing hepatocellular receptor

GPI: glycosyl phosphatidylinositol

RTK: receptor protein-tyrosine kinase

PCD: programmed cell death

TNFR: tumor necrosis factor receptor

dsRNA: double stranded ribonucleic acid

siRNA: small interfering ribonucleic acid

FACS: fluorescence activated cell sorting

RT-PCR: reverse transcription-polymerase chain reaction

GFP: green fluorescent protein

DAPI: 4',6-diamidino-2-phenylindole

LIST OF FIGURES / LIST OF TABLES

CHAPTER 1: INTRODUCTION

Mouse Embryonic Stem Cells

Embryonic stem (ES) cells are "pluripotent" cells meaning that in theory they are able to differentiate into any tissue or cell type, as opposed to "multipotent" cells which have lineage restriction to differentiate to cell types within the same progenitor type*(1)* . In 1908, the Russian scientist Alexander Maksimov assigned the term "stem cell" to describe cells that had "self-renewal" properties, progressing through numerous cycles of cell division while preserving their original or undifferentiated state*(2)* . In 1981 the first mouse embryonic stem cells (mESCs) were extracted from the inner cell mass (ICM) of a mouse embryo*(3, 4)* . In 1998, the embryonic stem cell line was revealed as a revolutionary scientific platform for their ability to accurately illustrate developmental processes in vitro*(5)* . Thompson and his team used donated human embryos, originally intended for in vitro fertilization, to conclude that the high telomerase activity exhibited in stem cells contributes to their infinite replicative life span*(5)* .

Today, targeted ES cell differentiation for the generation of new neurons holds excellent promise for those diagnosed with degenerative brain disorders such as Alzheimer's or Parkinson's disease*(6, 7)* . In addition, because stem cells can be grown indefinitely in culture, they can serve as a cost effective model for studying developmental processes. Finally, new possibilities have arisen from the potential ability

to repair damaged neural tissue by using embryonic stem cells to generate neural stem cells[8].

The differentiation of stem cells into neurons has been optimized using a monolayer differentiation protocol developed by Austin Smith[9]. Typically, when stem cells are allowed to freely differentiate into other cell types in culture, the outcome can yield variable and heterogeneous outcomes. However, this in vitro differentiation protocol generates cells in high yield that are broadly of forebrain fate. This method not only allows the study of neurogenesis in vitro at single cell resolution but also provides a platform to examine intrinsic and extrinsic mechanisms involved in neural specification provided by signaling[10-12].

<u>Neurogenesis and the Role of Ephrins</u>

The initial stage of vertebrate neurogenesis includes the induction and patterning of a neuron forming or neurogenic region along the primitive streak, followed by the birth and migration of neurons and glial cells (Figure 1) [13]. Next, axonal growth cones migrate towards their designated targets and subsequently form synaptic connections[14]. Many regions of the brain, including the cortex, develop in a layer-specific manner[15-18]. The layer in which a neuron resides is closely matched with its birth in comparison to neurons in other layers[19]. For instance, the oldest neurons can be found in the deepest cortical layer whereas youngest neurons exist in the outermost layer[20, 21]. One can confirm the layer fate of a specified neuron by examining the expression of genes in that layer specific region[22].
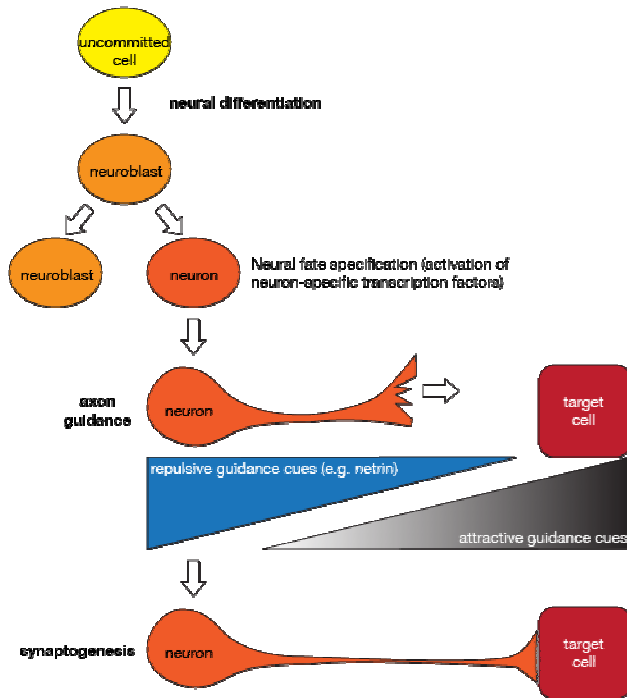
FIGURE 1: Stages of Neurogenesis

The first stage of neurogenesis is the induction and patterning of a neurogenic regions and specification of cell fates. The second stage is the birth and migration of neuron and glial cells. This is followed by guidance of axonal growth conges to form synaptic connections.

During brain development, many regions of the brain connect in a topographic manner, i.e. adjacent neurons in one region maintain their neighbor-neighbor relationship when they extend axons into another region *(23)* . Responsibility during this stage of neurogenesis is allocated to the Eph receptor tyrosine kinases and their cognate ephrin ligands. These are expressed in gradients, and utilize signaling to serve as positioning labels for the refinement of this neural map *(24, 25)* .

Ephrin signaling Erethropoeitin-producing hepatocellular (Eph) receptors are the largest known family of receptor protein-tyrosine kinases (RTKs) and function via direct cell-cell interaction with their cognate ephrin ligand*(26)* . Eph/ephrin signaling is required for multiple aspects of central nervous system development including mediation of axon guidance by forward signaling or promotion of angiogenesis for the distribution of the blood supply*(14, 27)* . The ephrins and their EphR receptors are categorized into two main classes based on sequence homology and structural composition, EphA and

EphB. The ephrins are composed of GPI anchored ephrin-A ligands and single-pass transmembrane ephrin-B ligands (Figure 2).

FIGURE 2: Structure and sequence homology of the Eph receptor and ephrin families

Structural elements include: Cys-rich, a unique cysteine rich domain found in the Eph receptors; FNIII, fibronectin type III motif; TM, transmembrane domain; GPI, glycosyl phosphatidylinositol membrane anchor; Core, a conserved core sequence in the ligands containing four invariant cysteines.

Ephrin-As have a high affinity for EphA receptors and ephrin-Bs typically bind EphB receptors, although some promiscuity does exist (Figure 3). For instance, evidence of cross reactivity has been published where ephrin-A5 binds to and activates the EphB2 receptor(28) . Examples of signaling capabilities include ephrin-A signaling pathways that are responsible for integrin function and Ephrin-B/EphB interactions that create the cell-cell repulsion that allow for organization of hindbrain segments(29, 30) . Ephrin-B2 is also responsible for axon retraction in retinal ganglion cells from distinct retinal regions(31) . Post-embryonically, ephrin signaling plays roles in synaptic plasticity, nerve regeneration, cancer progression, and pathological angiogenesis (32-35) .

EphR signaling can repulse axons from inappropriate target fields (Figure 1). EphRs and ephrins can also engage in bi-directional signaling. Forward signaling occurs when the ephrin sends positive cues to the receptor-bearing cell, whereas reverse signaling occurs downstream in the ligand-bearing cell. Reverse signaling is still not completely understood but what has been determined is that once activated, can be

4

responsible for the opposite reaction such as growth cone extension instead of the typical growth cone collapse*(31, 36)* .
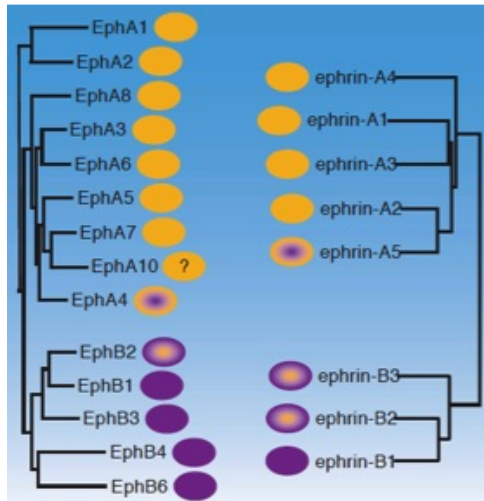
FIGURE 3: **Binding interactions between ephrins and their receptors**

Dual colored indicates cross reactivity with the opposing classes. For example, ligand ephrin-A5 primarily interacts with the EphA family of receptors (yellow), although it more weakly interacts with the EphB family of receptors (purple). EphA10 specific binding partner has yet to be determined*(35)*.

As mentioned previously, connectivity mapping during the development of the visual cortex also relies on signaling from ephrins *(37)* . Also, negative signaling cues provided by EphrinA2 can regulate proliferation in addition to controlling the approximate number of neural cells in the progressing brain*(38)* . Finally, ephrin signaling is implicated in controlling growth cones and cortical column formation*(39, 40)* . In summary, the organization of the nervous system during early development relies heavily on signaling from EphRs and ephrins, playing critical roles in proper cortical development, axon guidance, apoptosis, and cell polarity*(41-44)* .

Apoptosis in Early Neurogenesis

During mammalian development, the elimination of cells by programmed cell death (PCD) is a necessary event that allows multicellular organisms to regulate cell numbers to remove cells that are functionally redundant*(45)* . Apoptosis can also eradicate cells that are potentially detrimental to the organism*(45)* . In addition to

providing positive or negative directional cues for axon outgrowth, ephrin signaling is also required in apoptotic pathways to regulate brain size. Typically, programmed cell death (PCD) or apoptosis is required during normal mammalian development as a pruning mechanism to remove unnecessary structures, for example by removing skin between fingers and toes for segmented digits*(46)* .

Ephrin signaling is essential to balance the size of the neural progenitor cell population in early neurogenesis. Furthermore, over-activation of EphA signaling in vivo increases the rate of apoptotic death*(47, 48)* . The mechanism for which apoptosis is initiated by ephrins is not fully understood although one recent study indicated that EphA7 was physically associated Caspase-8 to induce apoptosis*(49)* . Furthermore, EphA7 is co-localized with tumor necrosis factor receptor 1 (TNFR1) on the cell surface, a well-known player in the extrinsic apoptosis pathway *(49)*. This interaction is lost once TNFR1 undergoes endocytosis, which confirms that apoptosis is initiated once EphrinA5 binds to EphA7 and activates the death receptor TNFR1 by physical association*(50)* . Additional results from an in vivo study have shown that together, ephrinA5 and EphA7 may function to balance cortical apoptosis to control overall neuronal mass*(43)* . This article demonstrated that over-expression of ephrinA5, driven from the EphA7 promoter, can lead to increased apoptosis. In addition, ephrinA5/A2 double mutant mice can display a reduction in apoptosis during neural patterning*(43)* .

Based these in vivo results, we set out to explore whether EphA signaling has a role in neuroblast apoptosis during in vitro differentiation. The hypothesis is that (1) Eph receptor and ephrin expression is conserved in vitro during the stem cell-to-forebrain

6

differentiation and (2) EphR/ephrin signaling is functioning to balance apoptosis during neural development.

In this study an in vitro system utilizing a stem cell-to-forebrain model with two different stem cell lines, Sox1-GFP and Oct4-GFP, was used to monitor the stem cell-to-neuron transition while characterizing changes in apoptosis levels. Through the use of ezRNAi transfections, knockdown of EphA3, EphA4, and EphA7 receptor gene expression was monitored to evaluate which Eph receptor was contributing to the apoptotic effect individually. Findings from this project are the first in vitro assay allowing for visualization of how exactly EphA7 is participating in cortical maturation through apoptotic mechanisms.

CHAPTER 2. MATERIALS AND METHODS

Stem Cell Culture and Maintenance

The following mouse embryonic stem cell lines (mESCs) were used throughout the duration of these thesis studies; Oct4-GFP*(51)* and Sox1-GFP*(9)* (Figure 4). These cell types have been derived from the E14Tg2A cell line. Both cell types were propagated as feeder-free cultures on 0.1% gelatin-coated plastic in sterile-filtered Glasgow modified Eagles medium supplemented with 1mM Sodium Pyruvate, 2mM L-Glutamine, 1X non-essential amino acids, 0.05mM Beta-mercaptoethanol, 1X Penicillin/Streptomycin, and 10% fetal bovine serum. 2U/uL of leukocyte inhibitory factor was added to 50mL aliquots of filtered media prior to usage. 5ml cultures were seeded at 5×10^5 cells in T-12.5 flasks. These cultures were split every two days and counted; media was replaced with fresh media on non-split days.

GFP   Transmission   Overlay

Figure 4: GFP expression in undifferentiated vs. differentiated cells

Oct4-GFP stem cells (top row) are fluorescent and become non-fluorescent upon differentiation. Cells are shown prior to differentiation. Sox1-GFP cells (bottom row) are non-fluorescent as stem cells but express GFP during neural differentiation. Shown are Day 8 neuroblasts.
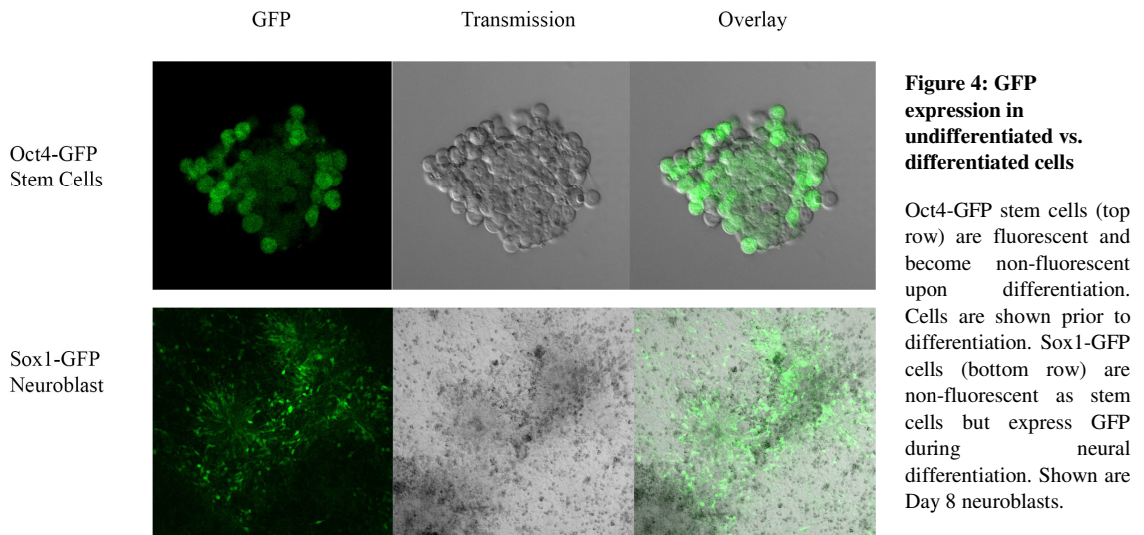
<u>Neural Differentiation</u>

Neuronal differentiation was carried out essentially as previously described *(9)* but with additional full volume media changes as necessary to remove cellular debris and dead cells. Differentiation was initiated at day 0 by plating stem cells on 0.1% gelatin-coated plastic surfaces at low density in N2B27 media. Seeding densities were as follows; $1.9x10^4$ cells per well of a 24-well plate or $2.1x10^5$ cells per 6cm plate. After 5 days post-differentiation, the cells were re-plated onto poly-ornithine and laminin-coated surfaces and seeded as follows; $3.8x10^4$ cells per well of a 24-well plate or $4.2x10^5$ cells per 6cm plate.

<u>Alternative Media and Differentiation Supplements</u>

An alternative to the Invitrogen supplied supplement is GEM 21 supplied by Gemini Biosciences. Neuroplex, which is compatible with the GEM 21 supplements, may be used in lieu of Neurobasal.

<u>Polymerase Chain Reaction (PCR)</u>

Forward and reverse primers for each fragment of the EphA receptors were designed by Bryan Lynn and ordered through Life Technologies (Appendix A). Polymerase chain reaction (PCR) was used to amplify 500-700bp fragments of each EphA receptor (EphA3, EphA4, or EphA7) that had been previously cloned into the pCR8/GW/TOPO plasmid by Cory Donelson (Figure 8). Second round PCR was used to extend a T7 promoter region onto the EphA receptor sequences for adequate transcription. The same was followed for attaching the T7 promoter region on the GFP cDNA sequence. The 2X primer mix contained Taq, dNTPs, and PCR buffer. Aliquots of

products (2uL each) were analyzed via 2% agarose gel in TAE buffer stained with
Ethidium Bromide.

Table 1: PCR Reaction Mix and Thermocycler Programming

PCR Reaction	Amount		Temp	Time
DI H_2O	9.5 uL		1) 94^OC	2 min
2X PCR Mix	12.5 uL		2) 94^OC	20 sec
F. Primer (10uM)	1.0 uL		3) 50^OC	30 sec
R. Primer (10uM)	1.0 uL		4) 72^OC	45 sec
PCR Template	1.0 uL		5) Go to #2	35 times
Total Mix	**25.0 uL**		6) 72^OC	5 min

RNA Transcription

In vitro RNA Transcription was carried out using the Ambion MEGA Script Kit
supplied by Life Technologies using the protocol and incubation temperatures outlined
below. Aliquots of products (1uL each) were analyzed via 2% agarose gel. The gel was
prepared with DEPC treated TAE buffer and Ethidium Bromide. Gel running conditions
were at 100 Volts in a DNase/RNase free environment (gel tank and running buffer).

Table 2: RNA Transcription Reaction Mix and Thermocycler Programing

Reaction	Amount		Temp	Time
DI H_2O	6.0 uL		1) 37^OC	4 hours
NTPs	8.0 uL		2) 90^OC	3 min
			3) -0.1^OC	3 min
10X Reaction Buffer	2.0 uL		4) 70^OC	3 min
			5) -0.1^OC	3 min
PCR Product DNA	2.0 uL		6) 50^OC	3 min
T7 Enzyme	2.0 uL		7) -0.1^OC	3 min
Total Mix	**20.0 uL**		8) 25^OC	3 min

Generation of siRNAs by RNase III Digest

The double stranded ribonucleic acid (dsRNA) products were digested with RNase III (New England BioLabs Inc.) to yield 20-23 base pair fragments of dsRNA or small interfering RNA (siRNA) according to the protocol outlined below[52] .

Table 3: RNase Digestion with NEB Shortcut RNase III

Reaction	Amount		Temp	Time
DEPC H$_2$O	65.0 uL		1) 37°C	30 min
dsRNA (20ug)	5.0 uL		2) 0°C	Place on Ice
10X NEB Buffer	2.0 uL		3) Add 10uL EDTA	Immediately
10X MnCl$_2$	2.0 uL		4) Purify	Immediately
NEB Shortcut RNase III	2.0 uL			
Total Mix	**100.0 uL**			

siRNA Purification

Fragmented siRNA was purified using RNA purification columns for small range RNA (Zymo Research). The procedure was performed as per the manufacture's protocol.

Transfections

For EphA receptor knockdown, purified siRNAs were transfected into cells using Lipofectamine 3000 (Life Technologies), 24 hours prior to analysis. Cells in culture were allowed to adhere on the gelatin coated surfaces for 24 hours prior to transfection. Cells in suspension were transfected directly into OPTIMEM and analyzed 24 hours later. pCAGGS-mCherry plasmid (kind gift of Bin Chen) was used as a co-transfection control to detect successful transfection of our RNAi constructs.

Table 4: Transfection with mCherry and siRNA Products

Reagent	Stock Concentration	Final Concentration/Well
Sham Transfected	Lipo 3000	2.0uL
GFP siRNA	265ng/uL	125ng, 250ng, or 500ng
mCherry Plasmid (Prep 1)	678ng/uL	
mCherry Plasmid (Prep 2)	179ng/uL	250ng, 500ng, or 1ug
EphA3 siRNA	365ng/uL	250ng or 500ng
EphA4 siRNA	119ng/uL	250ng or 500ng
EphA7 siRNA	566ng/uL	250ng or 500ng
Total Volume Transfected		**100uL/well**

Bioinformatics Assessment of Potential Cross-Binding

Basic Local Alignment Search Tool (BLAST) searches of the GFP siRNA products were analyzed for cross binding to mCherry (Appendix B)*(53)* .

Analysis of apoptosis by Annexin V binding and Flow Cytometry

Apoptosis was characterized at various timepoints ranging from Day 1 to Day 10 post-differentiation on the SH800 Sony Cell Sorter. Cells were lifted with Trypsin/EDTA and neutralized with 10% BSA/90% PBS. Cells were spun down and resuspended in 1X Binding Buffer (0.1M HEPES pH 7.4, 1.4M NaCl, and 25mM $CaCl_2$ in 1X PBS). 5uL of Cy5-labeled Annexin-V (BD Biosciences) was added to 100uL of resuspended cells for 15 minutes prior to adding 400uL of 1X Binding Buffer and analyzing by FACS. Annexin-V binds directly to phosphotidylserine, and can be used to indicate cells undergoing apoptosis versus necrotic cells. 25uL of a 5x 4',6-diamidino-2-phenylindole (DAPI) stain (1000X stock), used as a live/dead marker, was added to 100uL of resuspended cells and allowed to sit for 1 minute prior to analysis. Sox1-GFP and Oct4-

GFP stem cells were used as our differentiation trackers to identify the percentage of neuroblast cells in the population. Color compensation to remove spectral overlap between mCherry and Annexin was carried using Sony SH800 software by analyzing single color controls.

Confocal Microscopy

Cell morphology was analyzed at various time points ranging from Day 0 to Day 10 post-differentiation on a Zeiss LSM 700 confocal microscope. Post-transfection media was removed and cells were rinsed with PBS. 200uL of 1X Binding Buffer (0.1M HEPES pH 7.4, 1.4M NaCl, and 25mM $CaCl_2$ in 1X PBS) was added to each well. 10uL of Cy5-labeled Annexin-V (BD Biosciences) was added to 200uL of rinsed cells for 14 minutes prior to adding 50uL of 10X DAPI for an additional 1min. Solution was removed and cells were rinsed with PBS. 200uL of 1X binding buffer was added to each well then clusters of neuroblast were imaged. Oct4-GFP stem cells were used as our positive control. GFP was targeted for knockdown with GFP siRNA at concentrations of 125ng, 250ng, and 500ng per well. The corresponding % GFP expression was quantified by image analysis.

Ephrin and EphR Expression During in vitro Neurogenesis

        To answer the first question of whether or not Eph receptor and ephrin expression

is conserved in vitro during the stem cell-to-forebrain differentiation; expression of EphA

RTKs and their cognate ephrin-A ligands were examined. Quantification of mRNA levels

for EphAs and ephrin-As was performed (Figure 5). Using our stem cell-to-neural

differentiations, we can confirm that EphR and ephrin transcript levels seen in vitro

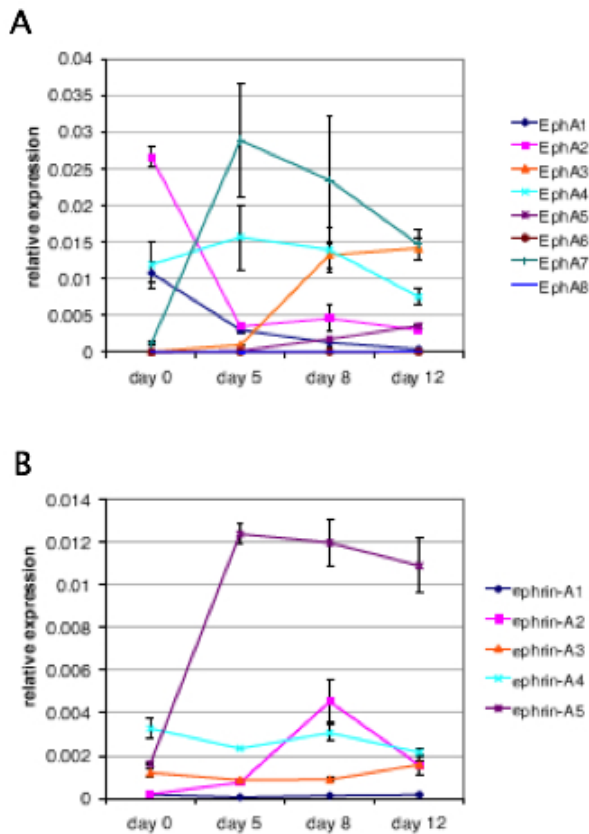broadly mirror previously published in vivo results *(9)* .

FIGURE 5: Quantification of RT-PCR profiles of EphA and ephrinA

(A) mRNA expression levels for EphA receptors. (B) mRNA levels of ephrin type A ligand expression. Data are plotted relative to beta-actin mRNA and is representative of three independent differentiation experiments. (Clay Hembree and Martin Hudson unpublished observations)

At day 0, EphA2 is highly expressed and drops to almost zero at day 5 and returns to midlevel from day 8 to day 12. EphA4 expression is maintained throughout neural differentiation. EphA7 expression is negligible at day 0, elevates to its highest peak at day 5 and steadily declines in expression throughout day 12 post-differentiation. EphA3 expression is first seen around day 8 and continues to day 12. EphrinA5 expression can be observed at day 5 post-differentiation and lingers until day 12. Overall, the expression levels seen in vitro correspond closely to expression profiles observed during forebrain development sequentially through time[11].

Oct4 is often used as a universal marker for stem cell fate and our data has shown loss of Oct4 at day 5 post differentiation (Figure 6A). This data has also indicated that at day 5 post-differentiation, the majority of the cell population has lost stem cell state and transformed into the desired neuronal fate, as demonstrated by high-level expression of the pro-neural transcription factor Sox1 (Figure 6B). Sox2 can serve as a stem cell marker but it also required in maintaining the cell's neural progenitor state. We observe a decrease around day 5, after which it maintains levels throughout the time points tested.

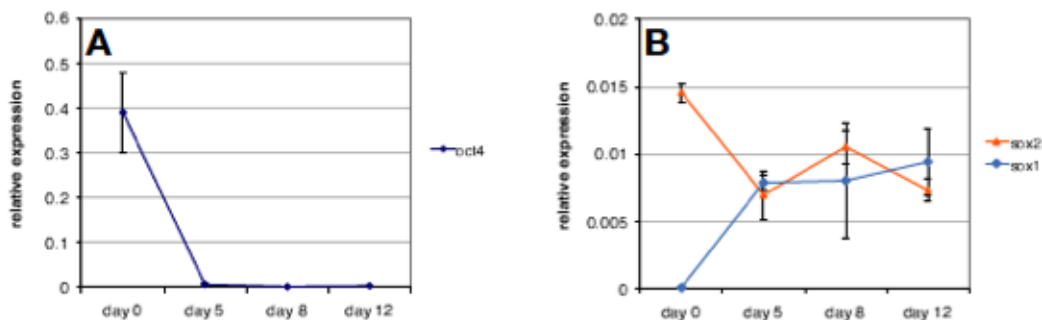
FIGURE 6: **Quantitation of RT-PCR profiles of stem cell and pro-neural markers**

(A) mRNA expression level of Oct4 showing a loss of expression at day 5. (B) mRNA levels of Sox1 (pro-neural marker) and Sox2 (stem cell marker). Data are plotted relative to beta-actin mRNA and is representative of three independent differentiations. (Clay Hembree and Martin Hudson unpublished observations)

The Sox1 pro-neural marker was expressed at constant levels throughout neural differentiation, from day 5 onwards. The loss of Oct4 by day 5 and the increase in expression of Sox1 agrees with other publications *(9, 54)* .

We used antibodies to demonstrate that EphA7 expression is detected in highest magnitude at the surface of in vitro-generated neural masses and decreasing in a gradient fashion towards the central most portion of the neural mass (Figure 7).   Because Nestin, which is a signature for neuroblast identity, and EphA7 are co-localized, this provides a good indication that EphA7 is expressed in developing neuroblasts*(55)* .   Although we see EphA7 expression in this cell type, we do not know what role Eph/ephrin signaling is playing during in vitro differentiation.
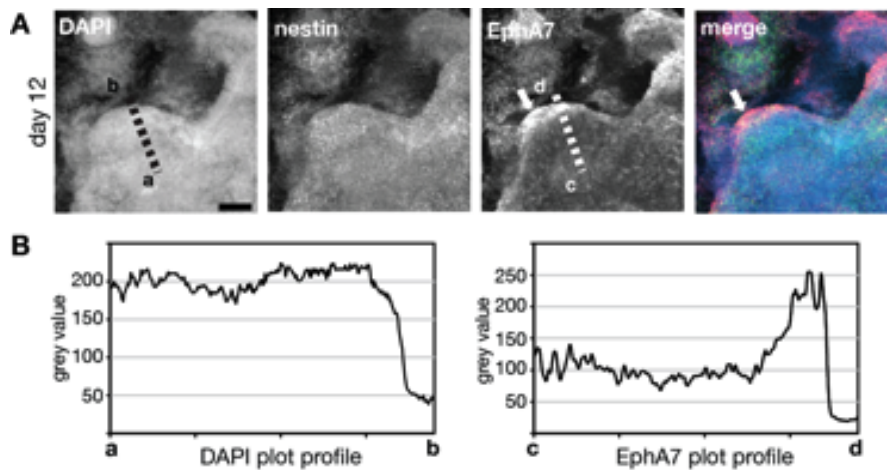

Figure 7: Distinct region of EphA expression in neural tissue

(A) Neural masses at differentiation day 12. The arrow indicates a EphA7 positive region located at the periphery. (B) EphA7 expression at the cross-section between point's m-n and p-q as noted on Figure 6A. (Clay Hembree and Martin Hudson unpublished observations)

Synthesis and Purification of EphA Receptor siRNA

Because the role of Eph/ephrin signaling during in vitro differentiation is not well understood, we used a knockdown system involving siRNA to expose the role of EphA7. Genetic mutations in the live mouse model are considered to be the gold standard for examining gene function in vivo. However, the average time to generate a mouse knockout takes about 18 months, is quite costly and completely unfeasible in smaller university laboratories. Here, we implement an in vitro model, which uses siRNA to transiently knock down gene function allowing for a rapid, reliable, and cost-effective method that can be implemented in essentially any laboratory. Transfecting siRNAs for gene silencing is a powerful genetic manipulation tool(56) . The mechanism of siRNA works by eliciting destruction of targeted mRNA stands by binding to the complementary sequence promoting rapid destruction(52) . siRNAs were generated from cloned, non-overlapping, EphA receptor fragments. In addition, GFP siRNAs were generated for use in assay validation and controls.
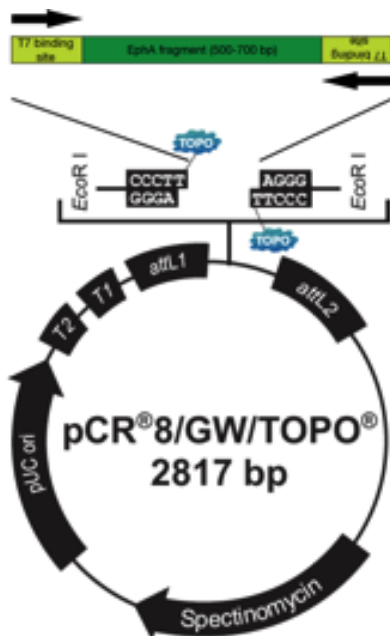

FIGURE 8: Plasmid for cloning EphA receptors

Polymerase chain reaction (PCR) was used to amplify the specified region portion of each EphA receptor (EphA3, EphA4, or EphA7), and a GFP cDNA sequence (Figure 8). This PCR step also allowed us to add a T7 RNA polymerase recognition site onto both ends of each fragment. Each DNA product was analyzed by agarose gel stained with Ethidium Bromide (Figure 9). Each cloned DNA fragment was a single band that indicates purity of each amplicon. The sizes were appropriate; EphA3 is 527 base pairs, EphA4 is 567 base pairs, EphA7 is 639 base pairs, and the GFP fragment is 750 base pairs in length.

The DNA fragments were then used as templates for *in vitro* transcription reactions to generate dsRNA (Figure 10), which was subsequently digested with RNase III, yielding 20-23 base pair fragments of dsRNA. These were purified using RNA purification columns. RNaseIII digestion was confirmed by agarose gel electrophoresis in RNase/DNase free environment (Figure 11). siRNA products were quantified via Nanodrop (Table 5). Due to the low yield of GFP siRNA, the dsRNA was re-digested and re-purified. It was concluded that preparation error had occurred because preparation 2 had adequate amounts of siRNA post-purification.
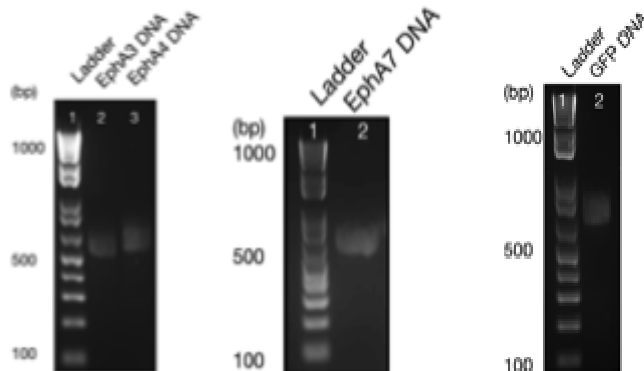
FIGURE 9: DNA Templates

Aliquots of products (2uL each) containing the T7 promoter site were analyzed via 2% agarose gel in TAE buffer stained with Ethidium Bromide.
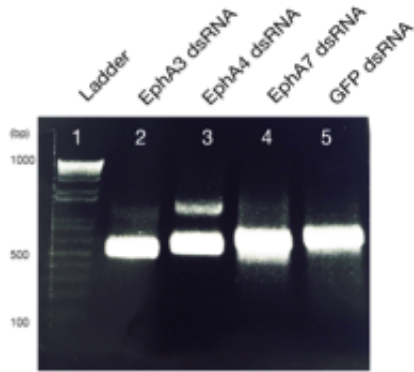
FIGURE 10: RNA Transcripts

Aliquots of dsRNA (2uL each) analyzed by 2% agarose gel in stained with Ethidium Bromide run in a DNase/RNase free environment. (Frank Tulenko and Marcus Davis unpublished observations)
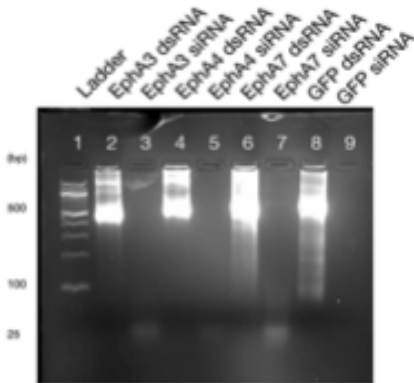
FIGURE 11: siRNA Products

Aliquots of purified siRNA (2uL each) analyzed by 3% agarose gel in stained with Ethidium Bromide. (Frank Tulenko and Marcus Davis unpublished observations)

Table 5: Nanodrop quantification of siRNA Products

<u>siRNA</u>	<u>Concentration</u>
EphA3	375ng/uL
EphA4	119ng/uL
EphA7	566ng/uL
GFP (Prep 1)	5ng/uL
GFP (Prep 2)	265ng/uL

Implementation of a Positive Control

To validate the siRNA delivery system, a GFP knockdown positive control was implemented. Initially a low dose (50ng) of GFP siRNA was transfected into Oct4-GFP stem cells and a time-course was applied to test the limits of the knockdown effect

(Figure 12). The 50ng concentration was selected based upon previously published data[57].

GFP Knockdown Timecourse

Y-axis: % GFP Expressing Cells (0 to 100)

Bars:
- 0ng GFP 24hrs: 81.3
- 50ng GFP 24hrs: 81.1
- 50ng GFP 48hrs: 77.3
- 50ng GFP 72hrs: 71.1
- 50ng GFP 96hrs: 63.5
- 50ng GFP 120hrs: 66.3

X-axis: Timecourse
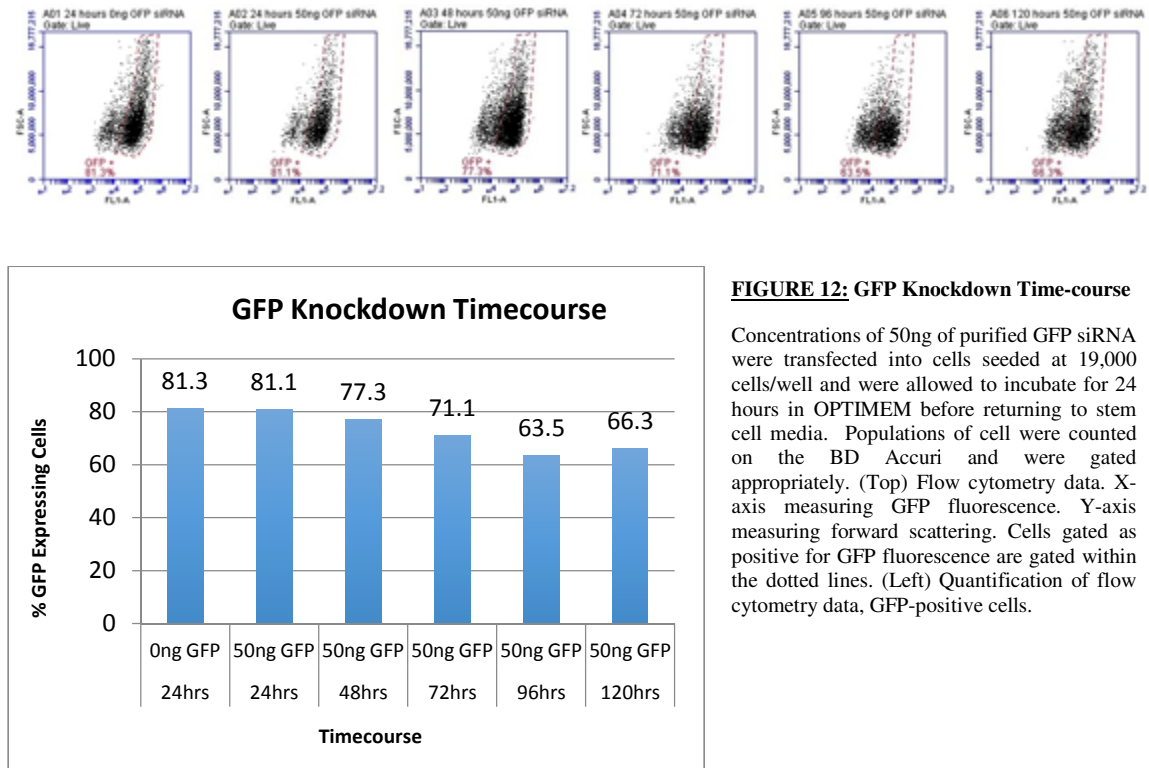
FIGURE 12: GFP Knockdown Time-course

Concentrations of 50ng of purified GFP siRNA were transfected into cells seeded at 19,000 cells/well and were allowed to incubate for 24 hours in OPTIMEM before returning to stem cell media. Populations of cell were counted on the BD Accuri and were gated appropriately. (Top) Flow cytometry data. X-axis measuring GFP fluorescence. Y-axis measuring forward scattering. Cells gated as positive for GFP fluorescence are gated within the dotted lines. (Left) Quantification of flow cytometry data, GFP-positive cells.

We observed a modest decrease in GFP expression after 96 hours post-siRNA transfection. However, because a dramatic knockdown effect was desired, the GFP siRNA was increased to concentrations of 125ng, 250ng and 500ng of siRNA per well. Phenotypic GFP expression was recorded through confocal microscopy to show the decrease in GFP fluorescing cells (Figure 13). This data was quantified by comparing total GFP fluorescence to total transmission data. From the results it is easy to conclude that a range of 125ng-500ng is sufficient to detect a concentration-dependent decrease in GFP fluorescence, so it was decided that 250ng of siRNA would be adequate to target EphA knockdown. At 500ng GFP siRNA threshold levels exceed the amount of lipofectamine and less siRNA is transfected, increase in GFP expression is observed.
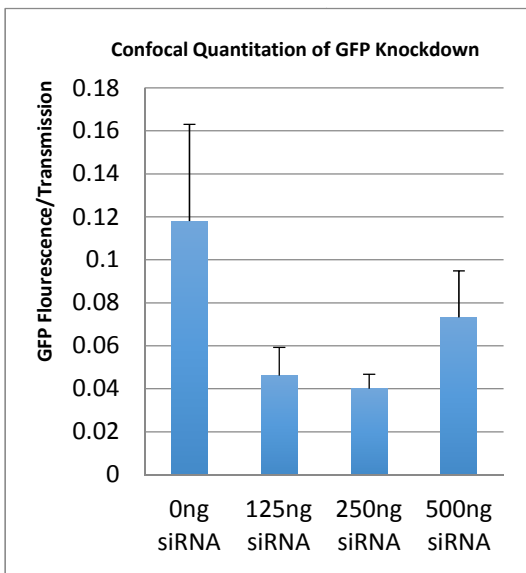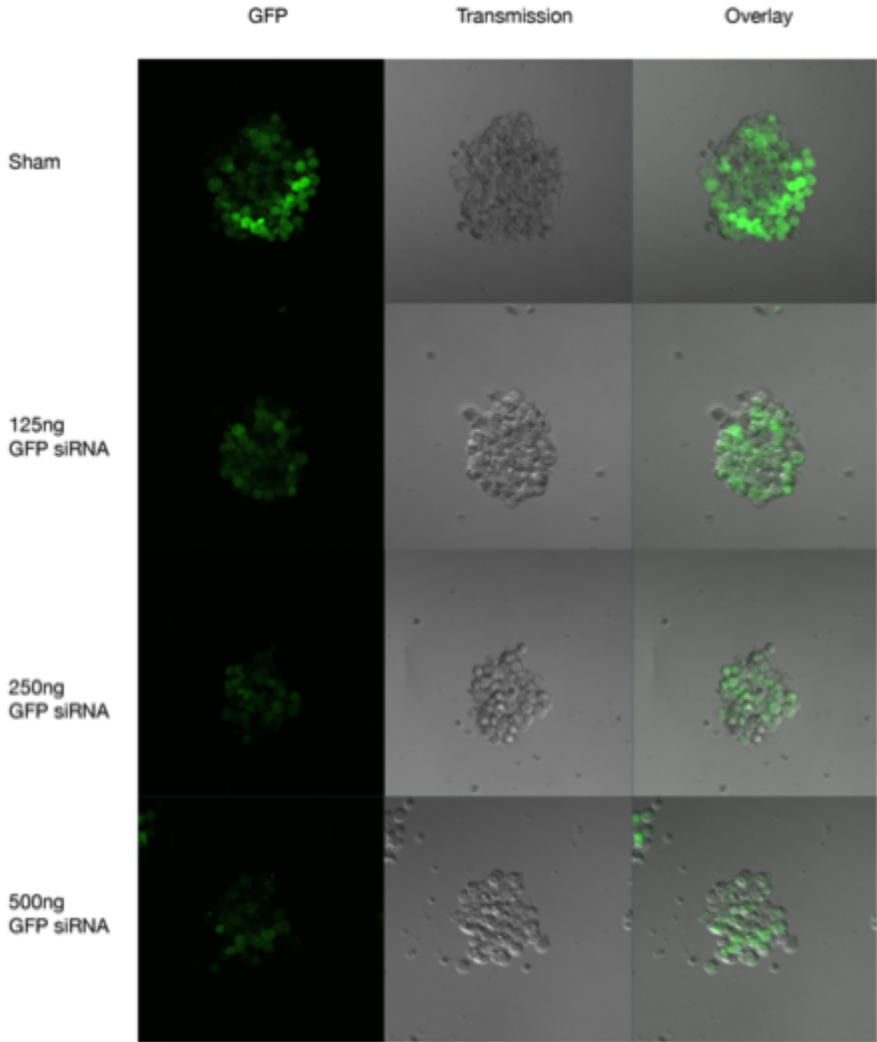
FIGURE 13: Confocal analysis of GFP knockdown

Concentrations of 125ng, 250ng, and 500ng of GFP siRNA were transfected into cells 24 hours prior to analysis. The Sham transfection was lipofectamine 3000 alone. Cell clusters for each condition were randomly selected for analysis. Measurements were calculated by dividing thresholded GFP fluorescence pixels by the total pixels in the cluster (measured from the transmitted light channel).

Co-Transfection Optimization

An mCherry co-transfection plasmid was used to detect successful transfection of the siRNA products. This will allow for selective gating to exclude untransfected cells from the population in evaluation. mCherry transfections were optimized in mESC media and OPTIMEM for stem cells and N2B27 and OPTIMEM for neurons (Figure 14). 750ng of plasmid was selected as a target range based upon recommendation by the Lipofectamine 3000 protocol. Throughout the transfection experiments, all of the cells were able to maintain resonable levels of viablity based on the percentage of live cells reported.

Stem cells were transfected with mCherry in both mESC media and OPTIMEM with about 30% transfection efficiency (Figure 14A). Therefore it can be concluded that stem cells posses the ability to be transfected in both stem cell media and OPTIMEM. Neurons were transfected with less efficiency in the OPTIMEM (13%) than the N2B27 media (24%). Based on the live cell population reported, the neuroblasts did not suffer from the OPTIMEM media, although rather less mCherry was taken up by the neuroblasts (Figure 14B).

Upon the deduction that stem cells are more easily transfected than neuroblasts (Figure 14C), it was recommended to use GFP siRNA knockdown on day 3 neuroblasts to test their ability to uptake GFP siRNA and to yield an observable reduction in GFP fluorescence (Figure 15). Cells were assessed 24, 48, and 72 hours after transfection. The experiment was set up in parallel with Day 0 stem cells for comparison purposes.
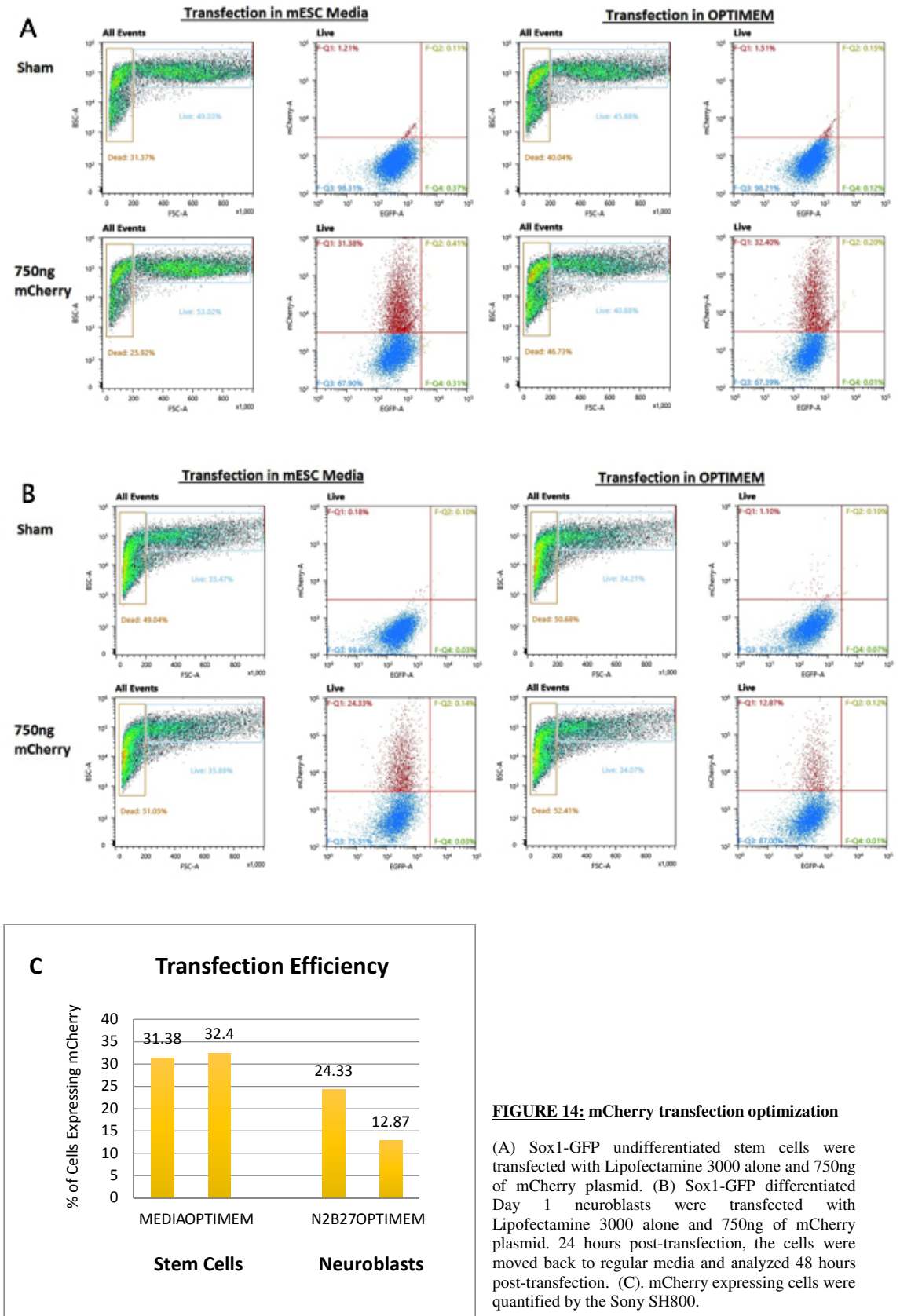
FIGURE 14: mCherry transfection optimization

(A) Sox1-GFP undifferentiated stem cells were transfected with Lipofectamine 3000 alone and 750ng of mCherry plasmid. (B) Sox1-GFP differentiated Day 1 neuroblasts were transfected with Lipofectamine 3000 alone and 750ng of mCherry plasmid. 24 hours post-transfection, the cells were moved back to regular media and analyzed 48 hours post-transfection. (C). mCherry expressing cells were quantified by the Sony SH800.

23
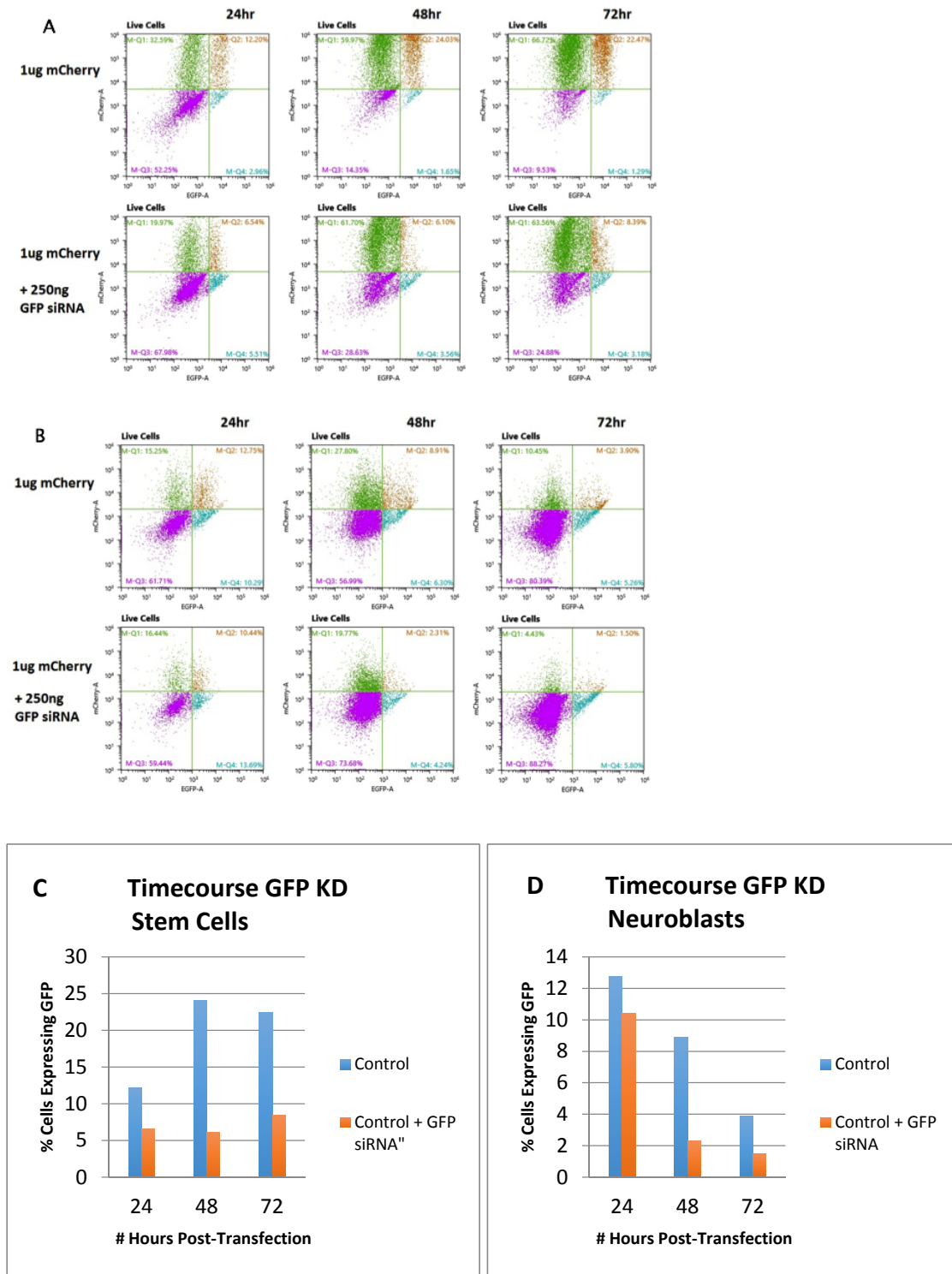
FIGURE 15: Comparison of GFP knockdown in Day 0 and Day 3 Oct4-GFP Cells

Cells were lifted and plated on gelatin-coated surfaces at 19,000 cells/well and allowed to settle for 24 hours prior to transfecting. Concentrations of 250ng of GFP siRNA along with 1ug mCherry were transfected into Oct4-GFP (A) day 0 stem cells or (B) day 3 neuroblast 24 hours prior to analysis. At 24 hours the OPTIMEM was removed and replaced with (A) stem cell or (B) N2B27 media respectively. (C) Quantified population of GFP positive stem cells and (D) population of GFP positive neuroblasts.

It was established that GFP knockdown was observed in both stem cells and neuroblasts and has a lasting knockdown effect out until 72 hours post-transfection. These finding suggest that mCherry can be considered a practical co-transfection control and that both stem cells and neuroblasts are susceptible to gene silencing via siRNA.

Apoptosis Method Validation

Flow cytometry was used to characterize apoptosis throughout the duration of this thesis. Apoptosis was assayed at various timepoints ranging from Day 1 to Day 10 post-differentiation, using both the BD Accuri flow cytometer and the Sony SH800 Cell Sorter. The Accuri automatically establishes laser and filter settings whereas the Sony requires some manual integration parameters to ensure optimal data collection.

The first step when working with the Sony is to calibrate with the negative control. Sox1-GFP day 0 stem cells were used as the negative control in these experiments because they contain no fluorophores. The cells were spun down and resuspended in 1X Binding Buffer and then each laser was set up to target the cell population in the center of the viewing window (Figure 16). Single color controls can be recorded to establish limits of detection for each fluorophore (Figure 17).
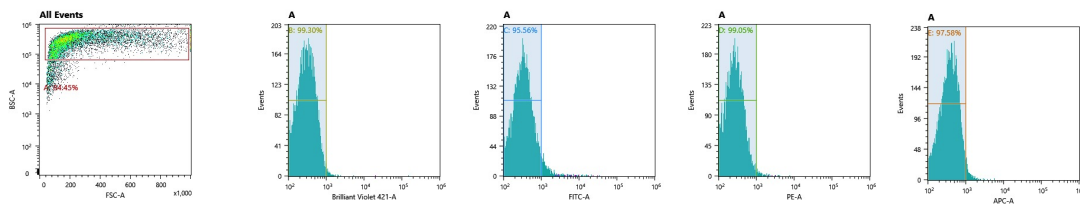
FIGURE 16: Gating for a negative control

Sox1-GFP stem cells were used to set up each laser setting. Brilliant Violet = DAPI (405nm), FITC = GFP (488nm), PE = mCherry (561nm), and APC = Cy5-Annexin (638nm).
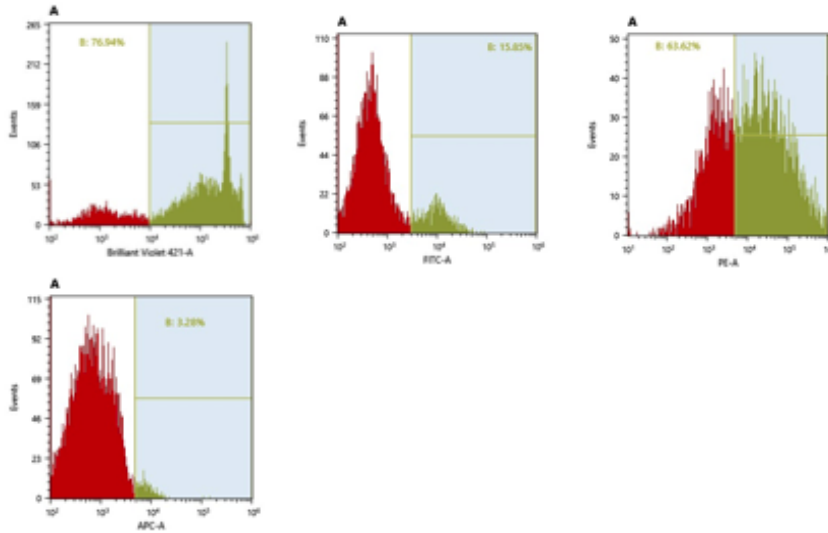
FIGURE 17: Gating for single color controls

(A) Brilliant Violet = DAPI (405nm) Sox1-GFP cells incubated with 1X DAPI for 1min. (B) FITC = GFP (488nm) Oct4-GFP Stem Cells. (C) PE = mCherry (561nm) Sox1-GFP stem cells transfected with mCherry Plasmid. (D) APC = Cy5-Annexin (638nm) Sox1-GFP Stem Cells incubated with 1X Cy5-Annexin for 15 minutes. Annexin-V binds directly to phosphotidylserine, and can be used to indicate cells undergoing apoptosis versus necrotic cells.

Automatic compensation can then be calculated using the gating from the negative control and single color controls. The resulting calculations are generated and can be applied to any subsequent data set (Figure 18). Occasionally manual compensation is required to fine-tune the removal of spectral overlap. In our case, incorporation of the mCherry co-transfection plasmid to detect successful transfection of our RNAi constructs, thought to be a useful efficiency control, led to complications. Unfortunately, the use of both mCherry and Annexin on the FACS required manual compensation due to major spectral overlap. Because of this, mCherry was not used in subsequent experiments.

Sample Group - 1 - Compensation Settings

Spillover Matrix (%)

Fluorochrome \ Detector	Brilliant Vio...	FITC	PE	APC	PerCP-Cy5.5	PE-Cy7
Brilliant Vio...	100.00	0.00	0.00	0.00	0.00	0.00
FITC	0.27	100.00	200.00	200.00	137.67	26.26
PE	0.01	3.14	100.00	47.83	16.96	3.25
APC	-0.01	-1.49	-1.47	100.00	47.48	7.67
PerCP-Cy5.5	0.00	0.00	0.00	0.00	100.00	0.00
PE-Cy7	0.00	0.00	0.00	0.00	0.00	100.00

Negative Value

Save | Load | Reset

Close
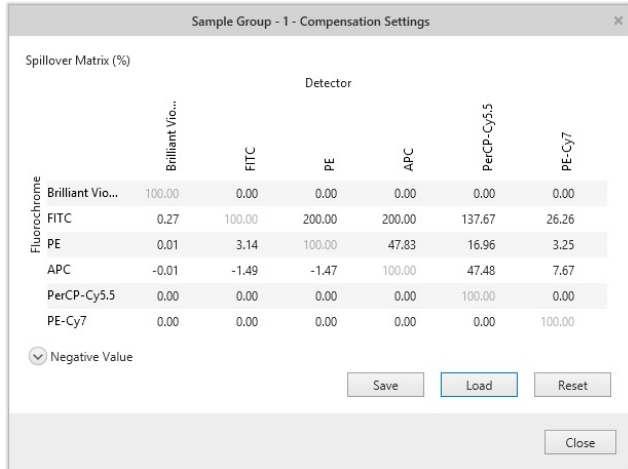
FIGURE 18: Automatic color compensation

The automatic color compensation matrix was calculated using single color controls.

mCherry expression is driven by the pCAGGS chicken actin promoter. This is a very strong promoter, which leads to very high expression levels of mCherry causing the signal to overpower that of the weaker Cy5 fluorophore. The major spectral overlap between mCherry and Annexin (Figure 19A) was accommodated via manual compensation (Figure 19B). Dragging the mCherry population back to its respective quadrant adjusted the color compensation matrix (Figure 19C).

A

■ Cy5 Excitation   ■ Cy5 Emission   ■ mCherry Excitation
■ mCherry Emission

B   Live Cells
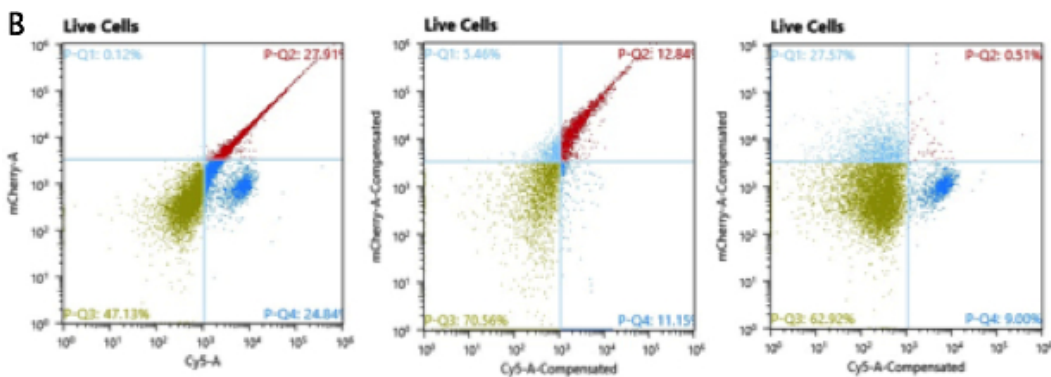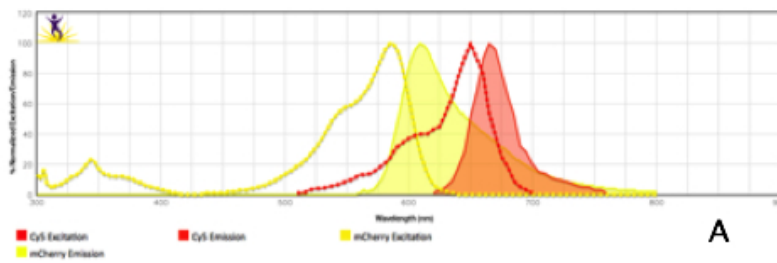
FIGURE 21: Applying Manual Color Compensation Calculation Matrix

(A) Spectral Overlap between mCherry and Cy5-Annexin in the emission spectra above, there is heavy spillover from mCherry channel into the Cy5-Annexin emission region. (B) Sample = Neuroblast mCherry Transfected Cells. (Left) No compensation applied. (Center) Results from Automatic compensation from single color control matrix. (Right) (C) Manual Compensation applied by dragging mCherry population back to the upper right quadrant where mCherry is gated appropriately.

In order to only account for live cells during the apoptosis assay, all dead cells need to be removed from the whole cell population in each individual sample. This was performed by incubating cells with 1X DAPI (4',6-diamidino-2-phenylindole) for 1 minute prior to analysis. Dead cells have ruptured membranes and are permeable to DAPI, which binds with high affinity to DNA whereas live cells exclude this dye. When viewed on a flow cytometry plot, the DAPI-stained population is clearly visible, allowing the operator to adjust the live/dead gate appropriately (Figure 20).
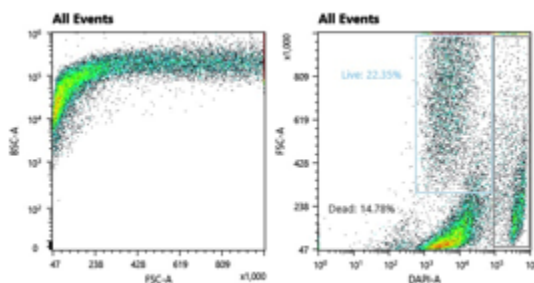
FIGURE 20: Live/Dead gating using DAPI

FSA = Forward scattering which measures the size of each individual cell as an event. BSC = Back scattering which measure cell complexity. (Left) Fragmented cells and cellular debris is found during events measuring less than 238 on the FSC horizontal axis. (Right) Cells staining positively for DAPI are gated appropriately and not factored into the live cell population.

The presentation of phosphatidylserine to the outer leaflet of the cell membrane is a characteristic hallmark of apoptosis. To determine the approximate number of cells undergoing apoptosis during the assay, cells were incubated with Cy5 labeled annexin V, which has a high binding affinity for phosphotidylserine. To validate our assay and

28

induce a major shift in the Cy5-Annexin V positive cell population, hydrogen peroxide (H_2O_2) was used to increase cellular stress and trigger apoptosis (Figure 21).
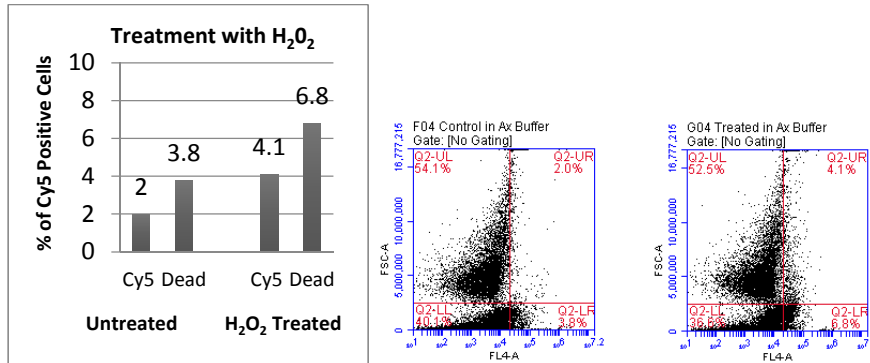
EphA Receptor Knockdown in Stem Cells

Investigation of the role of EphA receptors in stem cell maintenance was prompted by our observation that EphA4 is expressed in mESCs and throughout differentiation (Figure 2). This lead us to ask whether EphA3, EphA4 or EphA7 had any role in maintaining cells in the stem state. To address this, EphA3, EphA4, and EphA7 siRNAs were transfected into undifferentiated Oct4-GFP stem cells 24 hours prior to analysis (Figure 22).
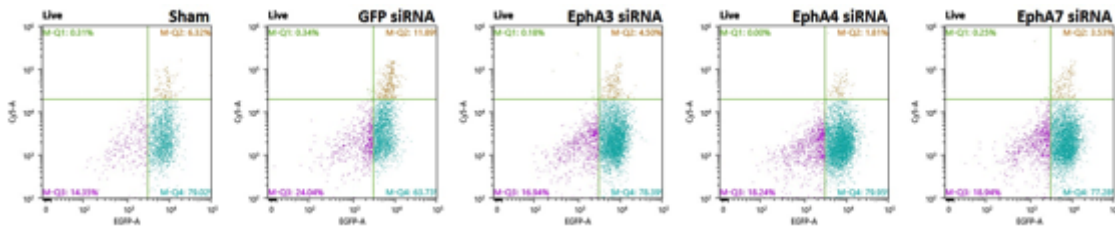
Sample	% Difference
Sham	0
GFP	16.9
EphA3	1.5
EphA4	3.1
EphA7	0.8

29
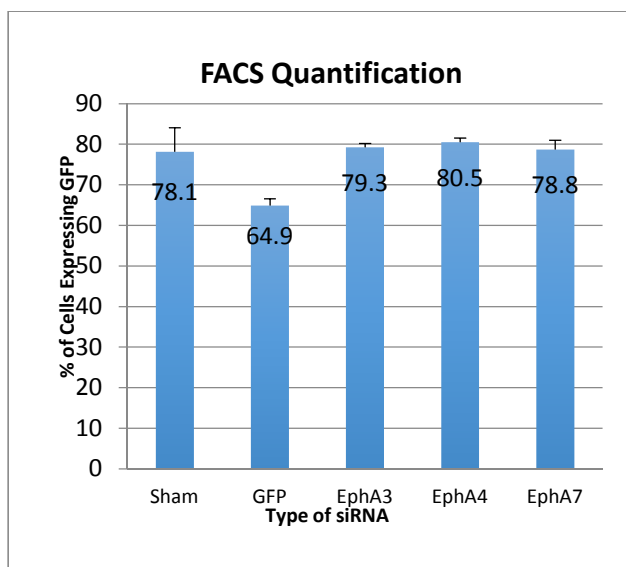
FIGURE 22: GFP knockdown on day 0 stem cells

Undifferentiated mouse embryonic stem cells were lifted and transfected in suspension with 500ng of siRNA and plated onto gelatin-coated wells of a 24-well plate. Cells were analyzed by FACS using DAPI staining for live/dead gating. Error bars are representative of experiment performed in triplicate.

The percent difference between the sham and the GFP siRNA transfected sample is about 17% thus confirming that the transfections had occurred. There is not a significant difference between the EphA siRNA transfected samples and the sham transfected. To increase the probability of observing a shift in GFP expression, mCherry was added to gate specifically for the siRNA transfected samples (Figure 23).
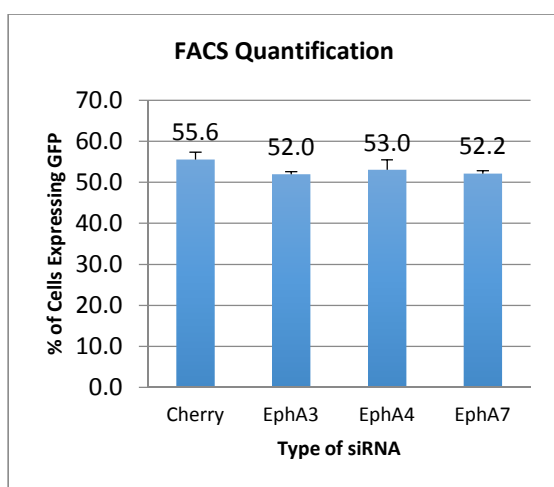
FIGURE 23: mCherry co-transfection with EphA siRNA in Oct4-GFP stem cells

Undifferentiated mouse embryonic stem cells were lifted and transfected in suspension with 250ng of EphA siRNA and 500ng of mCherry. Then plated onto gelatin-coated wells of a 24-well plate. Cells were analyzed by FACS using DAPI staining for live/dead gating. Error bars are representative of experiment performed in triplicate.

Oct4-GFP expression was maintained at about 80% throughout, irrespective of which EphA was knocked down (Figure 22) and even with transfection gate provided by

the mCherry co-transfection plasmid (Figure 23) there is not a dramatic difference between EphA KD GFP expressions. It can be concluded that EphA signaling has no obvious role in maintaining stem cell state.

Bioinformatics Assessment of Potential Cross-Binding

To ensure that transfected GFP siRNA was not knocking down our mCherry co-transfection control, we performed BLAST searches of the GFP siRNA products to analyze for possible cross binding to mCherry (See Appendix B)*(53)* . In order to achieve degradation of mRNA, 100% homology matching of 23 base pairs must be accomplished. Less than 100% may possibly provide disruption in translation but not necessarily targeted degradation. Cherry and GFP react at 100% with 23 base pairs and 100% with 18 base pairs. Keeping in mind that at 100% homology match for a 23 base pair fragment out of a possible 750 base pair length GFP fragment is about a 3% chance of providing a gene silencing effect. However, we may still observe an off-target effect from GFP to mCherry.

Alternative Media and Differentiation Supplements

A cost effective option to the Invitrogen supplied supplement is GEM 21 supplied by Gemini Biosciences. Differentiation was initiated at day 0 by plating cultured stem cells on 0.1% gelatin-coated plastic surfaces at low density in N2B27 media. An initial seeding density of 2.1×10^5 cells per plate was initiated on a total of 6x6cm plates.

However, we could not generate any viable neurons using this tissue culture supplement. The neurons when resuspended in GEM 21 N2B27 will adhere to gelatin-coated surfaces as normal but upon day 2 post-differentiation, they are struggling to

survive. In lieu of Neurobasal, Neuroplex, which is compatible with the GEM 21 supplements, was proven equivalent to the Neurobasal media during stem cell differentiations (data not shown).

EphA Receptor Knockdown in Neuroblasts

To test whether siRNA knockdowns were effective in neuroblasts, GFP, EphA3, EphA4, and EphA7 siRNA transfections were performed at Day 5 post-differentiation and analyzed by flow cytometry 24 – 72 hours later. The samples were run on both the Accuri (data not shown) and the Sony (Figure 24); both instruments yielded comparable results. We find that 72 hours post-transfection, apoptotic cells were around 8% of the entire cell population, and the only significant difference was the EphA7 siRNA transfected sample, which was 5.8% Cy5 positive. This result gave us insight that EphA7 knockdown resulted in a decrease of apoptotic cells in the sample population concluding that EphA7 plays a role in promoting apoptosis. Furthermore, EphA3 and EphA4 knockdown provided minimal changes in apoptosis levels indicating they play no roles in regulating cell progenitor pool size.

Apoptosis - Sony SH800
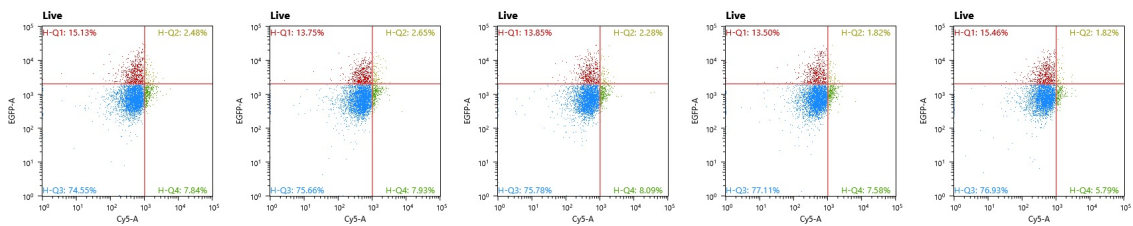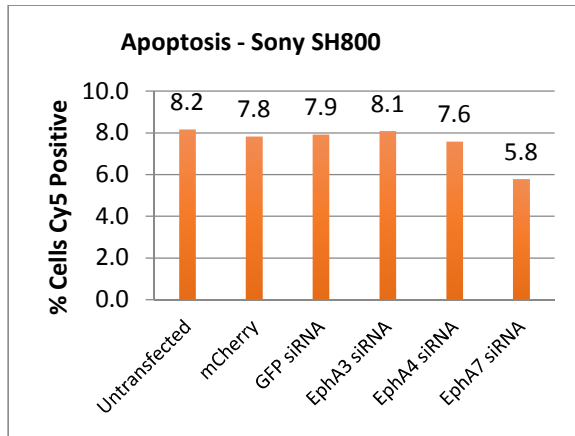
FIGURE 24: EphA knockdown in neuroblast

Sox1-GFP mouse embryonic stem cells were plated onto gelatin coated 6cm dishes at low density. At day 5 they were transfected in Optimem for 24 hours then the media replaced with N2B27 media. Cells were lifted and analyzed 72 hours post-differentiated.

We wanted to determine what time point gave us the best observation of apoptosis. To do this, we examined assayed for apoptosis at 24, 48, and 72 hours post-transfection. In this time course a gradual reduction in GFP expression was observed, which is to be expected of Oct4-GFP cells leaving the stem state and entering pro-neuronal fate (data not shown). The EphA7 siRNA transfected sample is a third less Cy5 positive than the mCherry transfected sample at 24 hours (Figure 25). However, at 48 and 72 hours post-transfection the EphA7 siRNA knockdown sample yields comparable levels of Cy5 positive cells when compared to the mCherry-transfected control. This suggests that 24 hours is optimal to view changes to apoptosis level due to EphA knockdown. At 48 and 72 hours post-knockdown, it is likely that the knockdown by siRNA is no longer effective (Figure 25). Whereas, at Day 5 EphA7 expression levels are maximal (Figure 2) and knockdown effects may take up to 72 hours to observe a shift in apoptotic activity (Figure 24).

Timecourse Apoptosis

Legend:
- Control
- Control + EphA7 siRNA

X-axis: # Hours Post-Transfection (24, 48, 72)
Y-axis: % Cells Cy5 Positive (0–35)
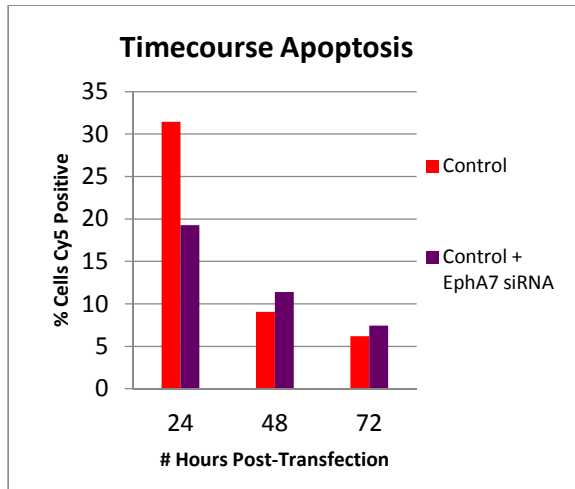
FIGURE 25: Day 3 neuroblasts knockdown time course

Oct4-GFP mouse embryonic stem cells were plated onto gelatin-coated surfaces at low density in N2B27 differentiation media. At day 3 they were transfected in optimem for 24 hours with EphA7 siRNA and a co-transfection control (mCherry). After 24 hours the cells were returned to N2B27 media. They were lifted and analyzed 24, 48, and 72 hours post-transfection. The samples were run on the SH800 and analyzed for apoptosis using Annexin-Cy5 staining.

Following out extensive method development, we assayed a single time point in triplicate using sham vs. EphA7 siRNA transfected samples. These were run without the mCherry co-transfection plasmid to remove any subjectivity involved with manual compensation. We found a 60% decrease in Cy5-AnnexinV stained cells after transfection with EphA7 siRNA when compared to sham-transfected controls (Figure 26). Student t-test of the two samples lead to a P value =0.0144. We conclude that apoptosis levels in EphA7 siRNA-treated cells are significantly different from sham controls. This data strongly suggest that EphA7 is playing a role in promoting apoptosis.
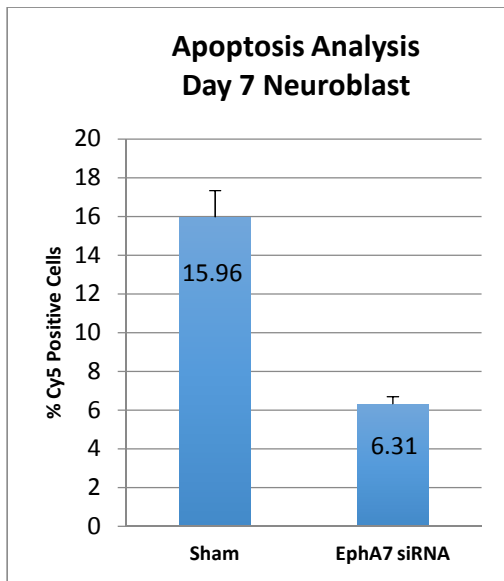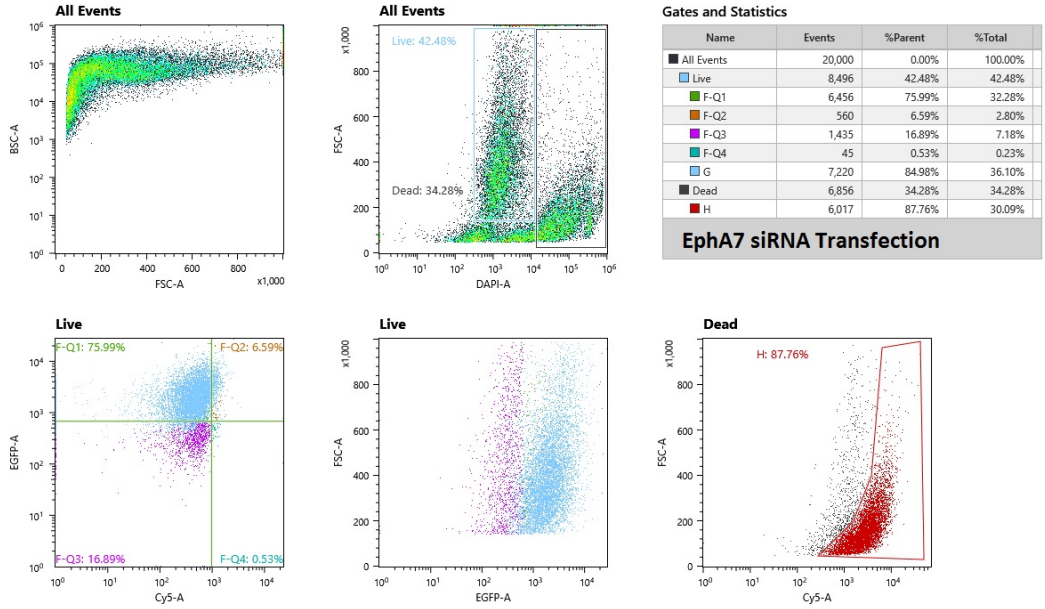
FIGURE 27: Apoptosis analysis on day 7 neuroblasts.

Day 6 neuroblast were lifted off laminin-coated surfaces, transfected in OPTIMEM and returned to laminin-coated wells of a 24-well plate. 24 hours post siRNA transfection; the cells were stained with Cy5-AnnexinV and DAPI then analyzed on the SH800 in triplicate. N = 3 experiments. Error bars are standard error of the mean.

CHAPTER 4. DISCUSSION

This thesis aimed to investigate the role of EphA receptor signaling in apoptosis during in vitro neurogenesis. Our original hypothesis was that (1) Eph receptor and ephrin expression is conserved during in vitro stem cell-to-forebrain differentiation and (2) EphR/ephrin signaling was functioning to balance apoptosis during neural development. The hypothesis was tested directly by developing an in vitro system using a stem cell-to-forebrain model with two different stem cell lines, Sox1-GFP and Oct4-GFP, to monitor the stem cell-to-neuron transition while characterizing changes in apoptosis levels. The Sox1-GFP cell line is a knock-in reporter ES cell line in which there is a random insertion of a Sox1 promoter driving GFP expression. In the neuroectoderm of the mouse embryo, Sox1 is the earliest marker of neural development *(58)* . The Oct4 gene was discovered as a primary maintenance gene to maintain stem cell pluripotency and gave rise to the Oct4-GFP mESC line in 2003 *(59, 60)* . Layer-specific cortical neurogenesis is conserved during embryonic stem cell to neuron differentiations*(61)* . Our qRT-PCR data support and extend these observations. In addition, we find that Eph and ephrin expression during in vitro differentiation broadly mirrors previously published in vivo data, further suggesting that we can recapitulate elements of cortical neurogenesis in vitro *(11)* .

An additional goal was to investigate if EphA receptors had any role in maintaining stem cell pluripotency. Currently there is no literature surrounding the idea that Eph/ephrin signaling is involved in maintaining stem cell pluripotent state. We chose

to investigate this because preliminary data shows EphA4 expression in mESCs and throughout differentiation (Figure 2). We found that Oct4-GFP expression was maintained at about 80% throughout, irrespective of which EphA was knocked down, suggesting that EphA signaling has no obvious role in the maintenance of stem cell fate. The inkling that EphR/ephrin signaling may be functioning in vitro to balance apoptosis during neural development was prompted upon discovery of a recent publication that displays an obvious reduction in apoptosis due to loss of EphA7 by mutation in an in vivo study(55) . This work demonstrates the significance of region-specific apoptosis involving ephrin signaling (55) . Data revealed in this thesis provides substantiating evidence that EphA7 knockdown led to a reduction in apoptosis levels during in vitro neural differentiation, indicating that EphA7 promotes apoptosis during in vitro neural differentiation. This concurs with data from an in vivo study that implicate ephrinA5 and EphA7 in balancing cortical apoptosis to control overall neuronal mass (43) . Additional support demonstrates that over-expression of ephrinA5, driven from the EphA7 promoter, can lead to increased apoptosis (62) .

We assayed apoptosis using flow cytometry. Cy5-labeled Annexin-V was used to quantify the cells undergoing apoptosis by binding to cell-surface phosphotidylserine. Also, DAPI staining was used to identify dead cells (which could potentially also display phosphatidyl serine on the cell surface) because it binds very quickly to dead cells' DNA by penetrating the partially ruptured cell membranes. This proved to be useful for live/dead gating of cell populations. In addition, incorporation of the mCherry co-transfection plasmid to detect successful transfection of our RNAi constructs was thought to be a useful efficiency control. Unfortunately, the use of both mCherry and Cy5-

AnnexinV on the FACS required the use of manual compensation due to major spectral overlap, hence mCherry was removed from subsequent experiments. mCherry is driven by the pCAGGS promoter, which is a very strong promoter, this lead to very high expression levels of the mCherry plasmid causing the signal to overpower that of the weaker Cy5 fluorophore.

Elaboration of a four-color fluorescent experiment enabled the ability to quantify cells in different stages of apoptosis and death in different cell populations. Transfecting siRNA for successful gene inhibition was proven as a practical method. Findings from this project allowed for visualization of how exactly EphA7 is participating in cortical maturation through apoptotic mechanisms.

CHAPTER 5. CONCLUSIONS AND FUTURE WORK

Conclusions

Because ephrins play a role in neurogenesis and literature has shown that they can control brain size in vivo, our ability to recapitulate these results during an in vitro study has proven to be valuable discovery that can contribute to scientific advancement. The primary objective of this thesis was to use a stem cell model of neural differentiation to determine if EphA3, EphA4, or EphA7 had any role in apoptosis during in vitro differentiation.

To investigate if EphA receptors had any role in maintaining stem cell pluripotency, EphA knockdown in Day 0 cells did not cause them to differentiate. The GFP expression in Oct4-GFP stem cells was maintained levels throughout the transfection with siRNA from EphA3, EphA4, and EphA7. This concluded that cells could still maintain their pluripotent state and resist differentiation during EphA receptor knockdown generating a negative result.

Knocking down GFP expression in Oct4-GFP stem cells and Sox1-GFP neuroblasts validated the siRNA transfection assays. We then assayed apoptosis during in vitro neural development by using ezRNAi transfections to knockdown of EphA3, EphA4, and EphA7 receptor expression. The knockdown of EphA3 and EphA4 had little to no effect on the number of Cy5 positive cells indicating that they have no role in the regulation of apoptosis during neuroblast differentiation. Finally, EphA7 knockdown lead to a reduction in apoptosis at all stages of neural differentiation assayed (day 3 through day 8). This finding confirms our original hypothesis to be correct.

Demonstrating that EphA7 receptor signaling plays a role in neuroblast survival during in vitro differentiation is a significant and novel body of research. Future findings may prove to be useful in the discovery and outline of more connections in other developmental processes as well as providing potential molecular targets for therapeutic applications in oncology*(63)* .

Future Work

Aside from what has been delineated in the finding of this thesis, additional experiments are worth mentioning in this chapter. One additional objective is to determine the mechanism of apoptosis triggered by Eph/ephrin signaling in vitro. Whether it is cross talk via death receptors or direct interaction with one or more of the caspases is not known and would make for a compelling future project.

Working with neural spheres in culture followed by Cryostat-sectioning and immunostaining for known apoptotic markers (e.g. cleaved caspase or TUNEL staining) could provide the opportunity to gain further insight into the role of apoptosis in neuronal precursor cells. This method allows for retention of neuronal morphology in relation to surrounding cells and may represent a closer in vitro approximation to in vivo neural development. For instance, by exploring neurospheres in culture we can examine the neuronal layering associated with in vivo cortical development.

Alternatively, by plating cells onto cover slips, we can assay for apoptosis via immunohistochemistry. We also plan to stimulate apoptosis using antibody-clustered EphrinA5 and expect to see an increase in apoptosis. Lastly, continuing research includes studying additional receptors, additional ligands, and/or additional timepoints.

REFERENCES

1. D'Amour, K. A.; Gage, F. H. Genetic and functional differences between multipotent neural and pluripotent embryonic stem cells. *Proc. Natl. Acad. Sci. U. S. A.* **2003***, 100 Suppl 1*, 11866-11872.

2. Konstantinov, I. E. In search of Alexander A. Maximow: the man behind the unitarian theory of hematopoiesis. *Perspect. Biol. Med.* **2000***, 43*, 269-276.

3. Evans, M. J.; Kaufman, M. H. Establishment in culture of pluripotential cells from mouse embryos. *Nature* **1981***, 292*, 154-156.

4. Martin, G. R. Isolation of a pluripotent cell line from early mouse embryos cultured in medium conditioned by teratocarcinoma stem cells. *Proc. Natl. Acad. Sci. U. S. A.* **1981***, 78*, 7634-7638.

5. Thomson, J. A.; Itskovitz-Eldor, J.; Shapiro, S. S.; Waknitz, M. A.; Swiergiel, J. J.; Marshall, V. S.; Jones, J. M. Embryonic stem cell lines derived from human blastocysts. *Science* **1998***, 282*, 1145-1147.

6. Lindvall, O.; Kokaia, Z. Stem cells for the treatment of neurological disorders. *Nature* **2006***, 441*, 1094-1096.

7. Sugaya, K.; Alvarez, A.; Marutle, A.; Kwak, Y. D.; Choumkina, E. Stem cell strategies for Alzheimer's disease therapy. *Panminerva Med.* **2006***, 48*, 87-96.

8. Temple, S. The development of neural stem cells. *Nature* **2001***, 414*, 112-117.

9. Ying, Q.; Stavridis, M.; Griffiths, D.; Li, M.; Smith, A. Conversion of embryonic stem cells into neuroectodermal precursors in adherent monoculture. *Nat. Biotechnol.* **2003***, 21*, 183-186.

10. Gaspard, N.; Vanderhaeghen, P. Mechanisms of neural specification from embryonic stem cells. *Curr. Opin. Neurobiol.* **2010***, 20*, 37-43.

11. Yun, M. E.; Johnson, R. R.; Antic, A.; Donoghue, M. J. EphA family gene expression in the developing mouse neocortex: regional patterns reveal intrinsic programs and extrinsic influence. *J. Comp. Neurol.* **2003***, 456*, 203-216.

12. O'Leary, D. D.; Nakagawa, Y. Patterning centers, regulatory genes and extrinsic mechanisms controlling arealization of the neocortex. *Curr. Opin. Neurobiol.* **2002***, 12*, 14-25.

13. Wilson, S. W.; Houart, C. Early steps in the development of the forebrain. *Developmental cell* **2004***, 6*, 167-181.

14. Egea, J.; Klein, R. Bidirectional Eph–ephrin signaling during axon guidance. *Trends Cell Biol.* **2007***, 17*, 230-238.

15. Sur, M.; Rubenstein, J. L. Patterning and plasticity of the cerebral cortex. *Science* **2005***, 310*, 805-810.

16. Vanderhaeghen, P.; Polleux, F. Developmental mechanisms patterning thalamocortical projections: intrinsic, extrinsic and in between. *Trends Neurosci.* **2004***, 27*, 384-391.

17. Rash, B. G.; Grove, E. A. Area and layer patterning in the developing cerebral cortex. *Curr. Opin. Neurobiol.* **2006***, 16*, 25-34.

18. O'Leary, D. D.; Chou, S.; Sahara, S. Area patterning of the mammalian cortex. *Neuron* **2007***, 56*, 252-269.

19. Van Den Ameele, J.; Tiberi, L.; Vanderhaeghen, P.; Espuny-Camacho, I. Thinking out of the dish: what to learn about cortical development using pluripotent stem cells. *Trends Neurosci.* **2014***, 37*, 334-342.

20. Leone, D. P.; Srinivasan, K.; Chen, B.; Alcamo, E.; McConnell, S. K. The determination of projection neuron identity in the developing cerebral cortex. *Curr. Opin. Neurobiol.* **2008***, 18*, 28-35.

21. Gaspard, N.; Vanderhaeghen, P. Laminar fate specification in the cerebral cortex. *F1000 Biol. Rep.* **2011***, 3*, 6-6. Epub 2011 Mar 1.

22. Molyneaux, B. J.; Arlotta, P.; Menezes, J. R.; Macklis, J. D. Neuronal subtype specification in the cerebral cortex. *Nature reviews neuroscience* **2007***, 8*, 427-437.

23. Tsuchida, T.; Ensini, M.; Morton, S.; Baldassare, M.; Edlund, T.; Jessell, T.; Pfaff, S. Topographic organization of embryonic motor neurons defined by expression of LIM homeobox genes. *Cell* **1994***, 79*, 957-970.

24. Flanagan, J. G. Neural map specification by gradients. *Curr. Opin. Neurobiol.* **2006***, 16*, 59-66.

25. Dufour, A.; Egea, J.; Kullander, K.; Klein, R.; Vanderhaeghen, P. Genetic analysis of EphA-dependent signaling mechanisms controlling topographic mapping in vivo. *Development* **2006***, 133*, 4415-4420.

26. Gale, N. W.; Yancopoulos, G. D. Ephrins and their receptors: a repulsive topic? *Cell Tissue Res.* **1997***, 290*, 227-241.

27. Cheng, N.; Brantley, D. M.; Chen, J. The ephrins and Eph receptors in angiogenesis. *Cytokine Growth Factor Rev.* **2002***, 13*, 75-85.

28. Himanen, J.; Chumley, M. J.; Lackmann, M.; Li, C.; Barton, W. A.; Jeffrey, P. D.; Vearing, C.; Geleick, D.; Feldheim, D. A.; Boyd, A. W. Repelling class discrimination: ephrin-A5 binds to and activates EphB2 receptor signaling. *Nat. Neurosci.* **2004***, 7*, 501-509.

29. Mellitzer, G.; Xu, Q.; Wilkinson, D. G. Eph receptors and ephrins restrict cell intermingling and communication. *Nature* **1999***, 400*, 77-81.

30. Huai, J.; Drescher, U. An ephrin-A-dependent signaling pathway controls integrin function and is linked to the tyrosine phosphorylation of a 120-kDa protein. *J. Biol. Chem.* **2001***, 276*, 6689-6694.

31. Petros, T. J.; Bryson, J. B.; Mason, C. Ephrin B2 elicits differential growth cone collapse and axon retraction in retinal ganglion cells from distinct retinal regions. *Developmental neurobiology* **2010***, 70*, 781-794.

32. Cortina, C.; Palomo-Ponce, S.; Iglesias, M.; Fernández-Masip, J. L.; Vivancos, A.; Whissell, G.; Huma, M.; Peiró, N.; Gallego, L.; Jonkheer, S. EphB–ephrin-B interactions suppress colorectal cancer progression by compartmentalizing tumor cells. *Nat. Genet.* **2007***, 39*, 1376-1383.

33. Ogawa, K.; Pasqualini, R.; Lindberg, R. A.; Kain, R.; Freeman, A. L.; Pasquale, E. B. The ephrin-A1 ligand and its receptor, EphA2, are expressed during tumor neovascularization. *Oncogene* **2000***, 19*, 6043-6052.

34. Lai, K.; Ip, N. Y. Synapse development and plasticity: roles of ephrin/Eph receptor signaling. *Curr. Opin. Neurobiol.* **2009***, 19*, 275-283.

35. Pasquale, E. B. Eph–ephrin promiscuity is now crystal clear. *Nat. Neurosci.* **2004***, 7*, 417-418.

36. Arvanitis, D.; Davy, A. Eph/ephrin signaling: networks. *Genes Dev.* **2008***, 22*, 416-429.

37. Cang, J.; Kaneko, M.; Yamada, J.; Woods, G.; Stryker, M. P.; Feldheim, D. A. Ephrin-as guide the formation of functional maps in the visual cortex. *Neuron* **2005***, 48*, 577-589.

38. Holmberg, J.; Armulik, A.; Senti, K. A.; Edoff, K.; Spalding, K.; Momma, S.; Cassidy, R.; Flanagan, J. G.; Frisen, J. Ephrin-A2 reverse signaling negatively regulates neural progenitor proliferation and neurogenesis. *Genes Dev.* **2005***, 19*, 462-471.

39. Pabbisetty, K. B.; Yue, X.; Li, C.; Himanen, J.; Zhou, R.; Nikolov, D. B.; Hu, L. Kinetic analysis of the binding of monomeric and dimeric ephrins to Eph receptors: correlation to function in a growth cone collapse assay. *Protein science* **2007***, 16*, 355-361.

40. Torii, M.; Hashimoto-Torii, K.; Levitt, P.; Rakic, P. Integration of neuronal clones in the radial cortical columns by EphA and ephrin-A signalling. *Nature* **2009***, 461*, 524-528.

41. Price, D. J.; Kennedy, H.; Dehay, C.; Zhou, L.; Mercier, M.; Jossin, Y.; Goffinet, A. M.; Tissir, F.; Blakey, D.; Molnár, Z. The development of cortical connections. *Eur. J. Neurosci.* **2006***, 23*, 910-920.

42. Chilton, J. K. Molecular mechanisms of axon guidance. *Dev. Biol.* **2006***, 292*, 13-24.

43. Depaepe, V.; Suarez-Gonzalez, N.; Dufour, A.; Passante, L.; Gorski, J. A.; Jones, K. R.; Ledent, C.; Vanderhaeghen, P. Ephrin signalling controls brain size by regulating apoptosis of neural progenitors. *Nature* **2005***, 435*, 1244-1250.

44. Joberty, G.; Petersen, C.; Gao, L.; Macara, I. G. The cell-polarity protein Par6 links Par3 and atypical protein kinase C to Cdc42. *Nat. Cell Biol.* **2000***, 2*, 531-539.

45. Twomey, C.; McCarthy, J. Pathways of apoptosis and importance in developement. *J. Cell. Mol. Med.* **2005***, 9*, 345-359.

46. Kerr, J. F.; Wyllie, A. H.; Currie, A. R. Apoptosis: a basic biological phenomenon with wide-ranging implications in tissue kinetics. *Br. J. Cancer* **1972***, 26*, 239-257.

47. Kuan, C.; Roth, K. A.; Flavell, R. A.; Rakic, P. Mechanisms of programmed cell death in the developing brain. *Trends Neurosci.* **2000**, *23*, 291-297.

48. Park, S. Brain-region specific apoptosis triggered by Eph/ephrin signaling. *Experimental neurobiology* **2013**, *22*, 143-148.

49. Lee, H.; Park, S.; Kang, Y. S.; Park, S. EphA Receptors Form a Complex with Caspase-8 to Induce Apoptotic Cell Death. *Mol. Cells* **2015**, *38*, 10.14348/molcells.2015.2279.

50. Lee, H.; Park, E.; Kim, Y.; Park, S. EphrinA5-EphA7 complex induces apoptotic cell death via TNFR1. *Mol. Cells* **2013**, *35*, 450-455.

51. Ying, Q.; Nichols, J.; Evans, E. P.; Smith, A. G. Changing potency by spontaneous fusion. *Nature* **2002**, *416*, 545-548.

52. Yang, D.; Buchholz, F.; Huang, Z.; Goga, A.; Chen, C. Y.; Brodsky, F. M.; Bishop, J. M. Short RNA duplexes produced by hydrolysis with Escherichia coli RNase III mediate effective RNA interference in mammalian cells. *Proc. Natl. Acad. Sci. U. S. A.* **2002**, *99*, 9942-9947.

53. Altschul, S. F.; Gish, W.; Miller, W.; Myers, E. W.; Lipman, D. J. Basic local alignment search tool. *J. Mol. Biol.* **1990**, *215*, 403-410.

54. Watanabe, K.; Kamiya, D.; Nishiyama, A.; Katayama, T.; Nozaki, S.; Kawasaki, H.; Watanabe, Y.; Mizuseki, K.; Sasai, Y. Directed differentiation of telencephalic precursors from embryonic stem cells. *Nat. Neurosci.* **2005**, *8*, 288-296.

55. Park, E.; Kim, Y.; Noh, H.; Lee, H.; Yoo, S.; Park, S. EphA/ephrin-A signaling is critically involved in region-specific apoptosis during early brain development. *Cell Death & Differentiation* **2012**, *20*, 169-180.

56. Ui-Tei, K.; Naito, Y.; Zenno, S.; Nishi, K.; Yamato, K.; Takahashi, F.; Juni, A.; Saigo, K. Functional dissection of siRNA sequence by systematic DNA substitution: modified siRNA with a DNA seed arm is a powerful tool for mammalian gene silencing with significantly reduced off-target effect. *Nucleic Acids Res.* **2008**, *36*, 2136-2151.

57. Takada, T.; Nemoto, K.; Yamashita, A.; Kato, M.; Kondo, Y.; Torii, R. Efficient gene silencing and cell differentiation using siRNA in mouse and monkey ES cells. *Biochem. Biophys. Res. Commun.* **2005**, *331*, 1039-1044.

58. Pevny, L. H.; Sockanathan, S.; Placzek, M.; Lovell-Badge, R. A role for SOX1 in neural determination. *Development* **1998**, *125*, 1967-1978.

59. Niwa, H.; Miyazaki, J.; Smith, A. G. Quantitative expression of Oct-3/4 defines differentiation, dedifferentiation or self-renewal of ES cells. *Nat. Genet.* **2000**, *24*, 372-376.

60. Niwa, H. How is pluripotency determined and maintained? *Development* **2007**, *134*, 635-646.

61. Gaspard, N.; Bouschet, T.; Hourez, R.; Dimidschstein, J.; Naeije, G.; Van Den Ameele, J.; Espuny-Camacho, I.; Herpoel, A.; Passante, L.; Schiffmann, S. N. An

intrinsic mechanism of corticogenesis from embryonic stem cells. *Nature* **2008**, *455*, 351-357.

62. Park, E.; Kim, Y.; Noh, H.; Lee, H.; Yoo, S.; Park, S. EphA/ephrin-A signaling is critically involved in region-specific apoptosis during early brain development. *Cell Death & Differentiation* **2013**, *20*, 169-180.

63. Trounson, A.; DeWitt, N. D. Stem cell biology: Towards the reality of cell therapeutics. *Nat. Cell Biol.* **2012**, *14*, 331-331.

APPENDIX A

mh844 Primer designs for ezRNAi   12.17.13   Products on intended target

---

>NM_010140.3 Mus musculus Eph receptor A3 (Epha3), mRNA

 product length = 527

Forward primer 1 GAGCGGAGCATGGTAACTTCT 21

Template   8 28

Reverse primer 1   TCGTGAACTGATGCTCTCGG 20

Template   534 515

Products on intended target

>NM_007936.3 Mus musculus Eph receptor A4 (Epha4), mRNA

 product length = 567

Forward primer 1   AGCAACTTGGTCTGCAAGGT 20

Template   2323 2342

Reverse primer 1   AACCACGGCTTCTAGTGTCG 20

Template   2889 2870

Products on intended target

>NM_010141.3 Mus musculus Eph receptor A7 (Epha7), transcript variant 1, mRNA

 product length = 639

Forward primer 1   AGGCTCTTCGCTGCTGTTAG 20

Template   1524 1543

Reverse primer 1   TGCACCAATCACACGCTCAA 20

Template   2162 2143

Primers (ordered 12.17.13)

EphA3F1   GAGCGGAGCATGGTAACTTCT

EphA3R1   TCGTGAACTGATGCTCTCGG

EphA4F1   AGCAACTTGGTCTGCAAGGT

EphA4R1   AACCACGGCTTCTAGTGTCG

EphA7F1   AGGCTCTTCGCTGCTGTTAG

EphA7R1   TGCACCAATCACACGCTCAA

Forward primer- 5' -TCACTATAGGGAGAG- original forward primer- gene-3'

Reverse primer-5' -TCACTATAGGGAGAC- original reverse primer-gene-3'

Redesigned primer set:

EphA3F1   **TCACTATAGGGAGAGGA**GCGGAGCATGGTAACTTCT

EphA3R1   TCACTATAGGGAGACTCGTGAACTGATGCTCTCGG

EphA4F1   TCACTATAGGGAGAGAGCAACTTGGTCTGCAAGGT

EphA4R1   TCACTATAGGGAGACAACCACGGCTTCTAGTGTCG

EphA7F1   TCACTATAGGGAGAGAGGCTCTTCGCTGCTGTTAG

EphA7R1   TCACTATAGGGAGACTGCACCAATCACACGCTCAA

APPENDIX B

BLAST ®

Basic Local Alignment Search Tool

GFP ⟶ cherry

Blast 2 sequences

Nucleotide Sequence (719 letters)

RID NU2THDE311N (Expires on 05-22 06:31 am)

Query ID	lcl|Query_48613	**Subject ID**	lcl|Query_48615
Description	None	**Description**	None
Molecule type	nucleic acid		See details
Query Length	719	**Molecule type**	nucleic acid
		Subject Length	813
		Program	BLASTN 2.2.31+

Graphic Summary

Distribution of 5 Blast Hits on the Query Sequence

Color key for alignment scores

<40	40-50	50-80	80-200	>=200

Query

1   100   200   300   400   500   600   700

52
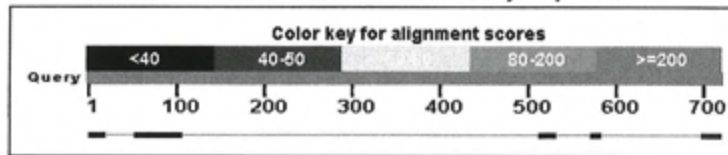
Dot Matrix View

Descriptions

Sequences producing significant alignments:

Description	Max score	Total score	Query cover	E value	Ident	Accession
None provided	42.8	168	17%	8e-08	100%	Query_48615

Alignments

Sequence ID: lcl|Query_48615 Length: 813 Number of Matches: 5
Range 1: 684 to 706

Score	Expect	Identities	Gaps	Strand	Frame
42.8 bits(46)	8e-08()	23/23(100%)	0/23(0%)	Plus/Plus	

Features:

```
Query  696  CGGCATGGACGAGCTGTACAAGT  718
            |||||||||||||||||||||||
Sbjct  684  CGGCATGGACGAGCTGTACAAGT  706
```

Range 2: 65 to 117

Score	Expect	Identities	Gaps	Strand	Frame
39.2 bits(42)	9e-07()	43/56(77%)	6/56(10%)	Plus/Plus	

Features:

```
Query  56   TGGACGGCGACGTAAACGGCCACAAGTTC---AGCGTGTCCGGCGAGGGCGAGGGC  108
            ||| | || | ||  |||||||||| ||||   | ||||| |||||||||||||||
Sbjct  65   TGGAGGGCTCCGTGAACGGCCACGAGTTCGAGATCGAG---GGCGAGGGCGAGGGC  117
```

Range 3: 1 to 18

Score	Expect	Identities	Gaps	Strand	Frame
33.7 bits(36)	4e-05()	18/18(100%)	0/18(0%)	Plus/Plus	

Features:

```
Query  4    GTGAGCAAGGGCGAGGAG  21
            ||||||||||||||||||
Sbjct  1    GTGAGCAAGGGCGAGGAG  18
```

Range 4: 304 to 324

Score	Expect	Identities	Gaps	Strand	Frame
30.1 bits(32)	5e-04()	19/21(90%)	0/21(0%)	Plus/Plus	

Features:

```
Query  511  AACATCGAGGACGGCAGCGTG  531
            ||| | |||||||||| |||||
Sbjct  304  AACTTCGAGGACGGCGGCGTG  324
```

Range 5: 405 to 416

Score	Expect	Identities	Gaps	Strand	Frame
22.9 bits(24)	0.071()	12/12(100%)	0/12(0%)	Plus/Plus	

Features:

```
Query  570  CGACGGCCCCGT  581
            ||||||||||||
Sbjct  405  CGACGGCCCCGT  416
```